Magnetic Force Microscopy (MFM)

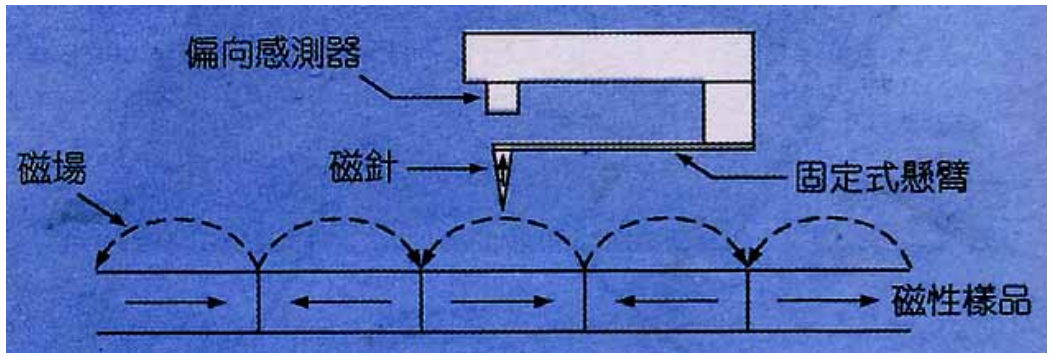

$$F = \mu_o(m \bullet \nabla)H$$

1. MFM is based on the use of a ferromagnetic tip as a local field sensor. Magnetic interaction between the tip and the surface results in a force acting on the tip, which can be detected from the deflection of the cantilever. Alternatively, the dynamic properties of the tip oscillation, i.e. amplitude, phase or frequency can be used. In this case, the observed signal is proportional to the derivative of the force.
2. The tip is scanned several tens or hundreds of nanometers above the sample, avoiding contact. Magnetic field gradients exert a force on the tip's magnetic moment, and monitoring the tip/cantilever response gives a magnetic force image. To enhance sensitivity, most MFM instruments oscillate the cantilever near its resonant frequency with a piezoelectric element. Gradients in the magnetic forces on the tip shift the resonant frequency of the cantilever. Monitoring this shift, or related changes in oscillation amplitude or phase, produces a magnetic force image.
3. Applications: magnetic recording media, micromagnetism, domain wall dynamics and pinning, failure analysis in electrical circuit, studies of superconducting current.

Magnetic Force Microscopy (MFM)

1. Magnetic force microscopy (MFM) images the spatial variation of magnetic forces on a sample surface. Resolution: 10~25 nm.
2. The system operates in non-contact mode. An image taken with a magnetic tip contains information about both the topography and the magnetic properties of a surface. Which effect dominates depends upon the distance of the tip from the surface, because the interatomic magnetic force persists for greater tip-to-sample separations than the van der Waals force. If the tip is close to the surface, in the region where standard non-contact AFM is operated, the image will be predominantly topographic. As the separation between the tip and the sample increases, magnetic effects become apparent.
3. A magnetizer is needed to magnetize the tip. Note that the structure of "soft" magnetic samples like Permalloy or garnet films can be significantly changed by the field of the tip that has a relatively high coercitivity. Tip-induced reorientation of surface magnetization and surface-induced reorientation of the tip magnetization can complicate the image interpretation.

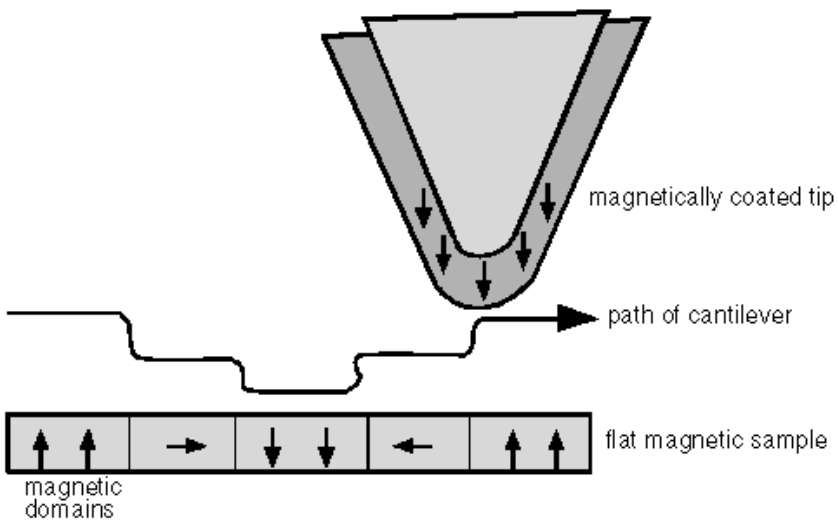

Lift Mode (MFM & EFM)

Since magnetic (electrostatic) forces can be either attractive or repulsive, problems with feedback loop stability in the non-contact imaging mode are likely to occur.

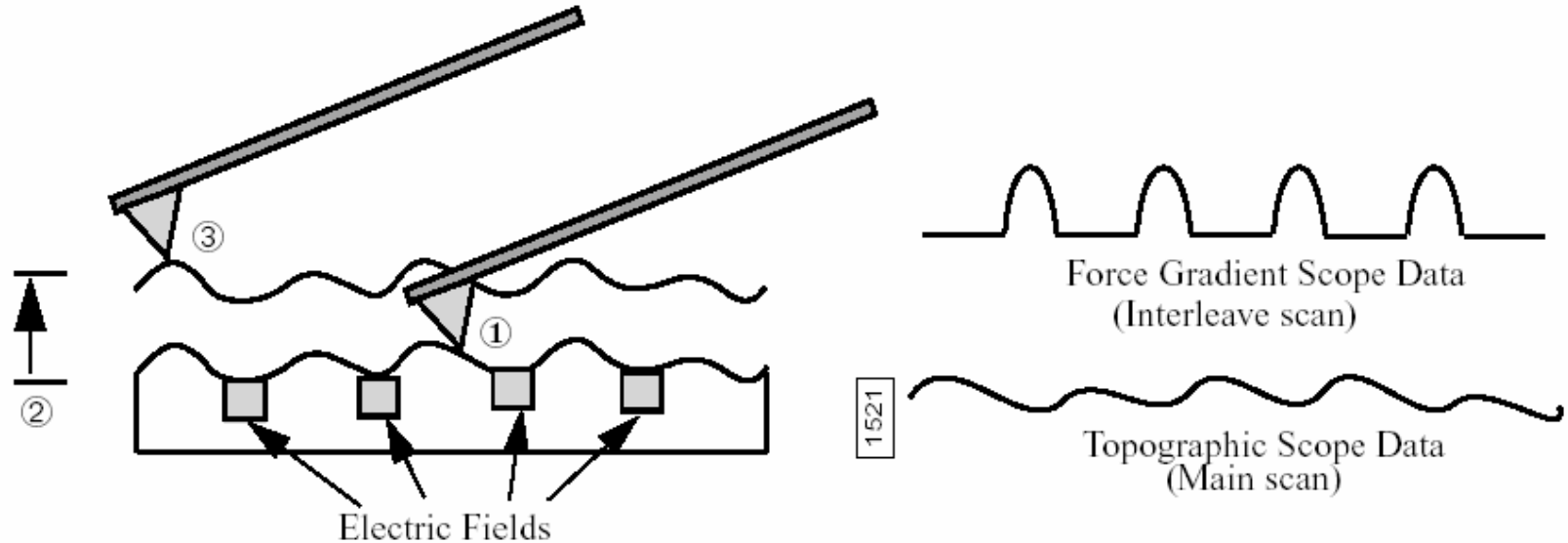

1. Cantilever measures surface topography on first (main) scan.

2. Cantilever ascends to lift scan height.

3. Cantilever follows stored surface topography at the lift height above sample while responding to magnetic (electric) influences on second scan (measured by amplitude, phase or frequency detection).

Magnetic Force Microscopy (MFM)

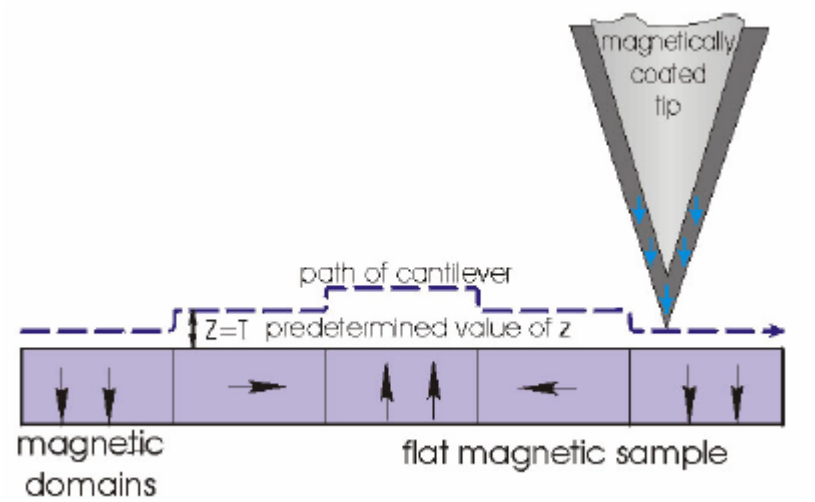

Topography

MFM

Magneto-
optical disk

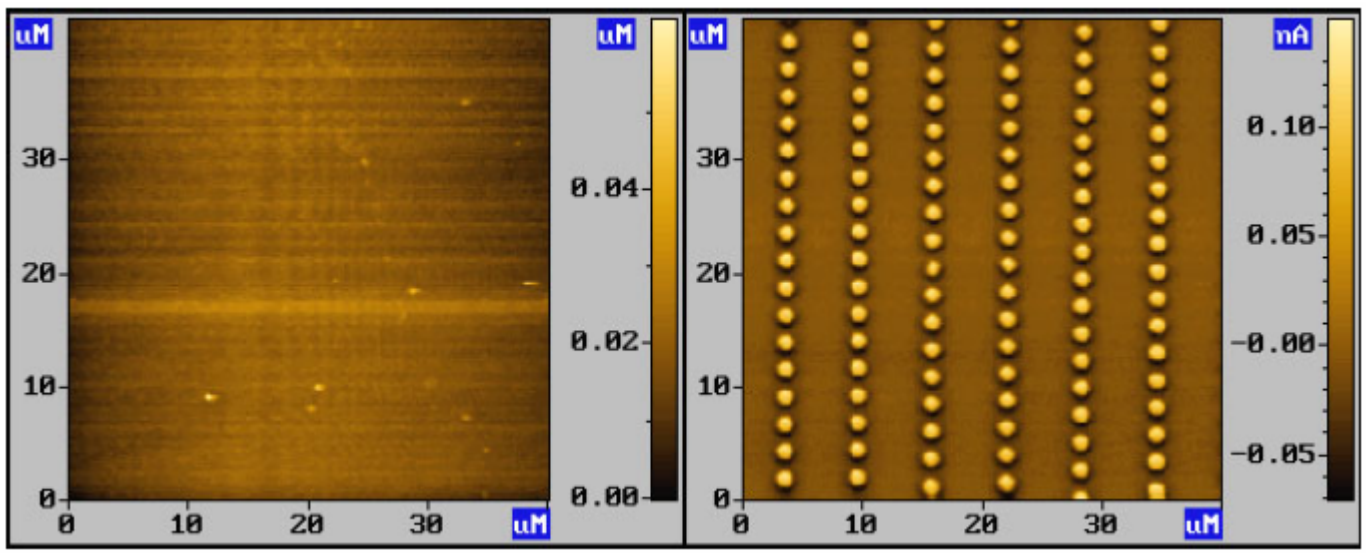

Tip-Surface Magnetic Forces

$$F = \mu_o(q + m\cdot\nabla)H$$

1. If the length of the effective domain at the tip apex is small compared to the characteristic decay length of the sample stray field, the tip can be approximated as point dipole. $F = \mu_o(m\cdot\nabla)H$ In this case, the gradient of the stray field in the vicinity of the surface rather than the field itself contributes to the force signal. Co tip.
2. For a large domain size, only the front part of the domain effectively interacts with surface stray field. $F = \mu_o qH$, the field is detected. Ni, Fe tips

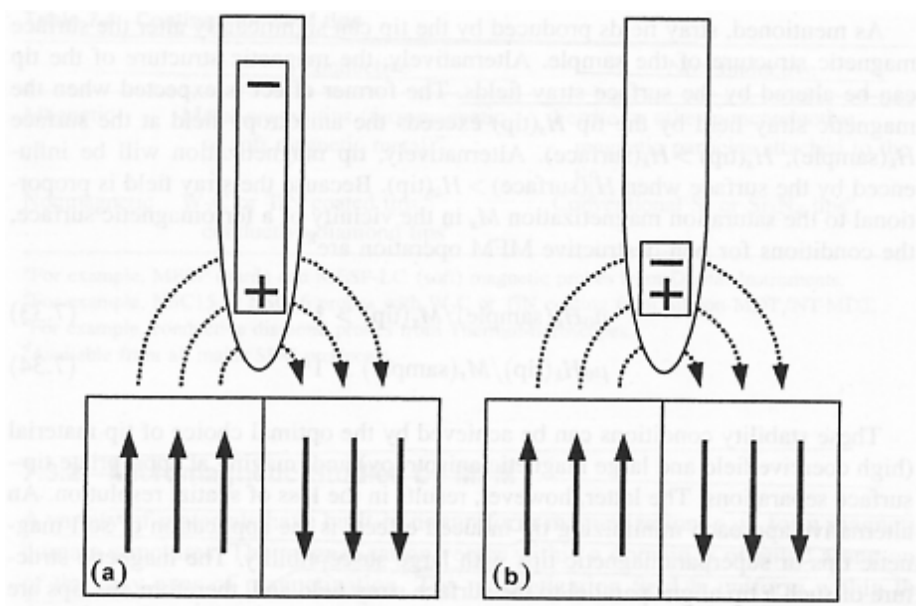

Figure 7.12. The origin of monopole and dipole terms in MFM imaging. **a**, the characteristic size of magnetic domain in the tip is much larger than the spatial extent of the surface stray field, the monopole term dominates. **b**, If the characteristic domain size in the tip is small, the dipolar term dominates. For a realistic tip shape both terms are present.

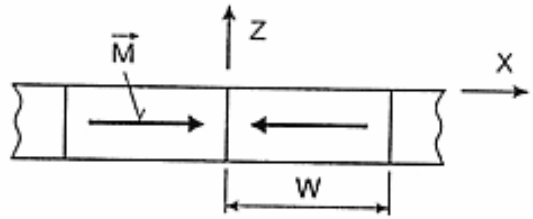

Co tip

(a)

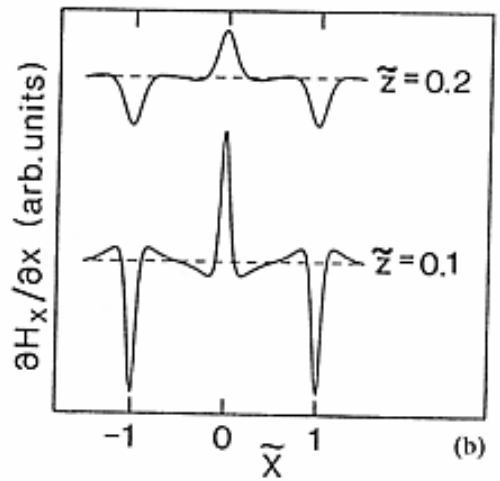

(b)

Ni tip

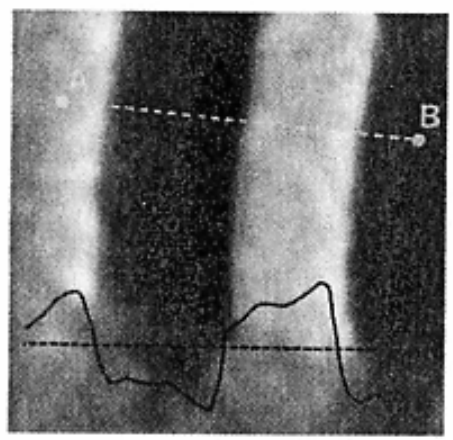

(c)

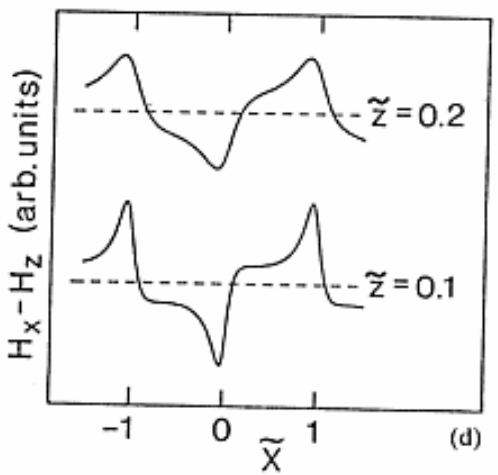

(d)

1. Quantification of MFM images is virtually impossible because the magnetic state of the tip is generally unknown.

2. The tip-induced reorientation of surface magnetization or surface-induced reorientation of the tip magnetization can be minimized by the optimal choice of the tip material (high coercive field and large magnetic anisotropy) and imaging at appropriate tip-surface separations. The latter, however, results in the loss of spatial resolution.

3. An alternative approach is the application of soft magnetic tips or superparamagnetic tips with large susceptibility. The magnetic structure of such a tip aligns parallel to the surface stray field and the tips are sensitive to the absolute value of magnetic field. $F = \frac{1}{2} \chi V \nabla B^2$
where χ is the magnetic susceptibility and V is the effective tip volume.

4. Interpretation of the MFM data from nonhomogeneous materials and current-carrying devices can suffer from electrostatic contributions to force or force gradient signal contrast, especially for conventional metal or metal-coated tips.

Domain Structure on (110) magnetite

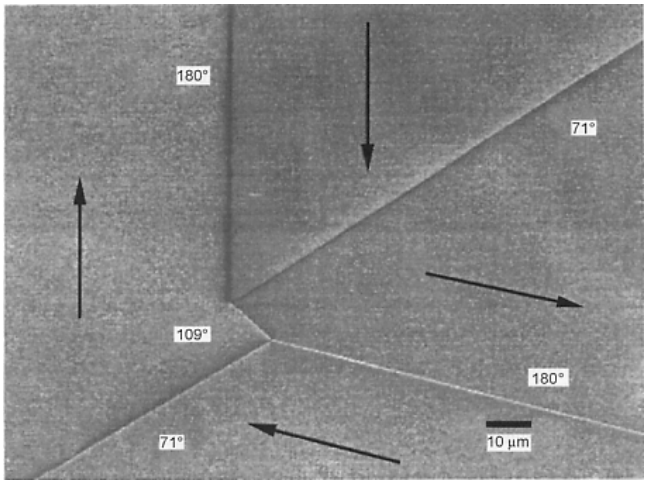

Tip Effect-decreasing the separation

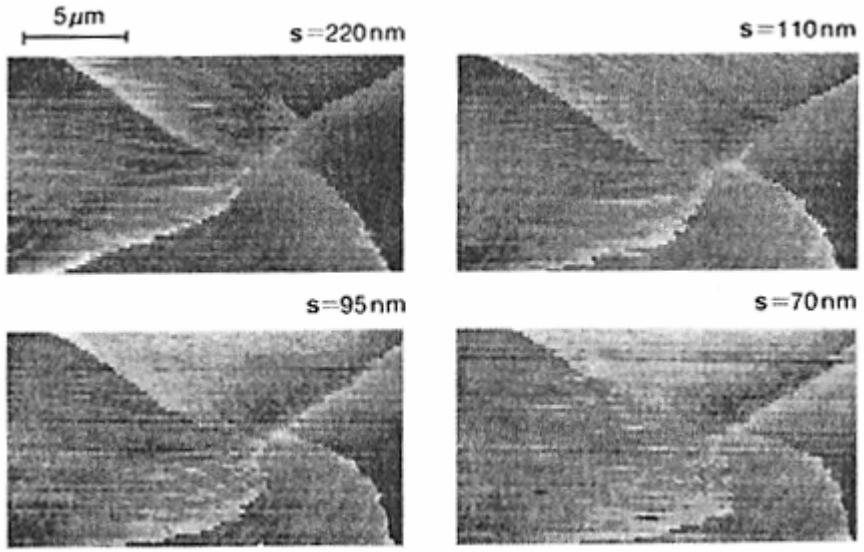

Fe films

90° Neel wall

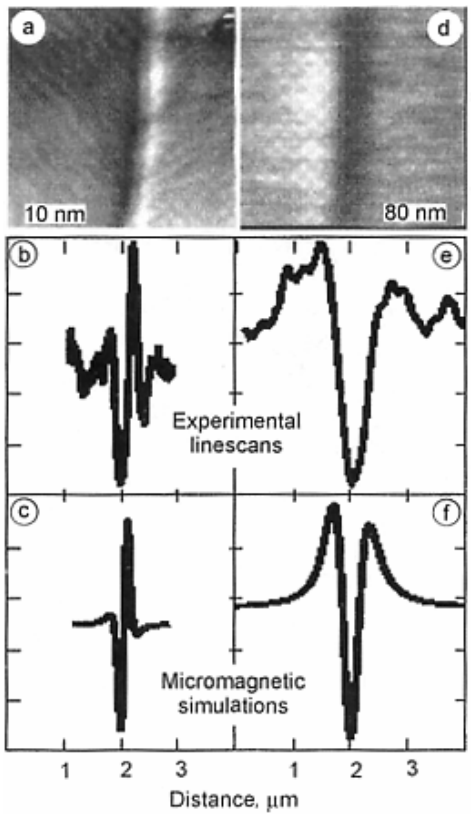

90° Bloch wall

910 nm

520 nm

390 nm

910 nm

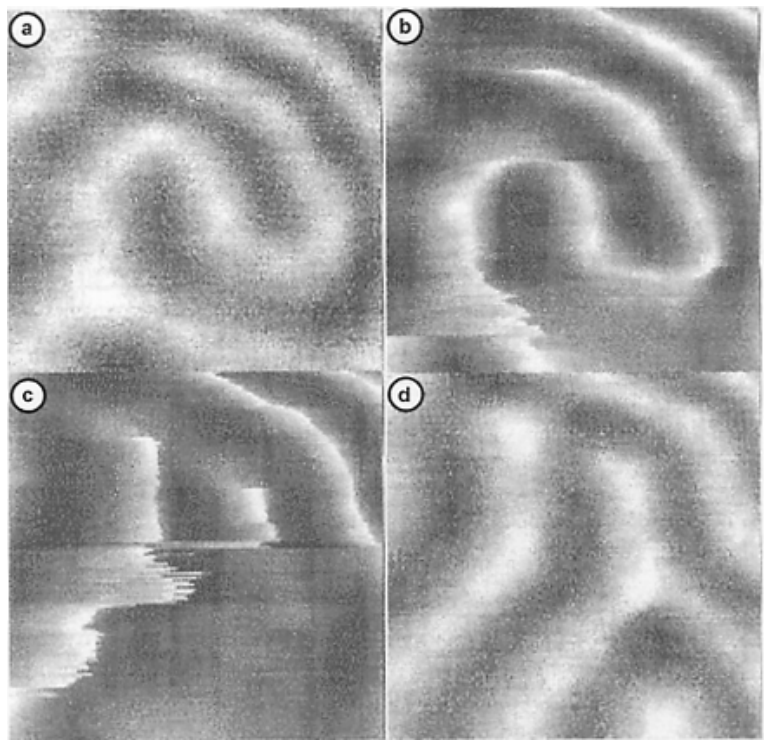

Electrostatic Force Microscopy (EFM)

Tip: Si cantilevers with conductive coating.

The grounded tip first acquires the surface topography using the tapping mode. A voltage between the tip and the sample is applied in the second scan (Lift-Mode 50 to 100 nm) to collect electrostatic data. EFM measures electric field gradient and distribution above the sample surface. EFM is used to monitor continuity and electric field patterns on samples such as semiconductor devices and composite conductors, as well as for basic research on electric fields on the microscopic scale.

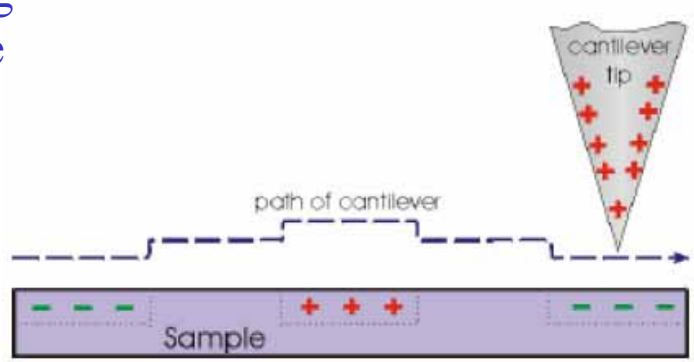

Topography

EFM

Metallic electrode under the voltage

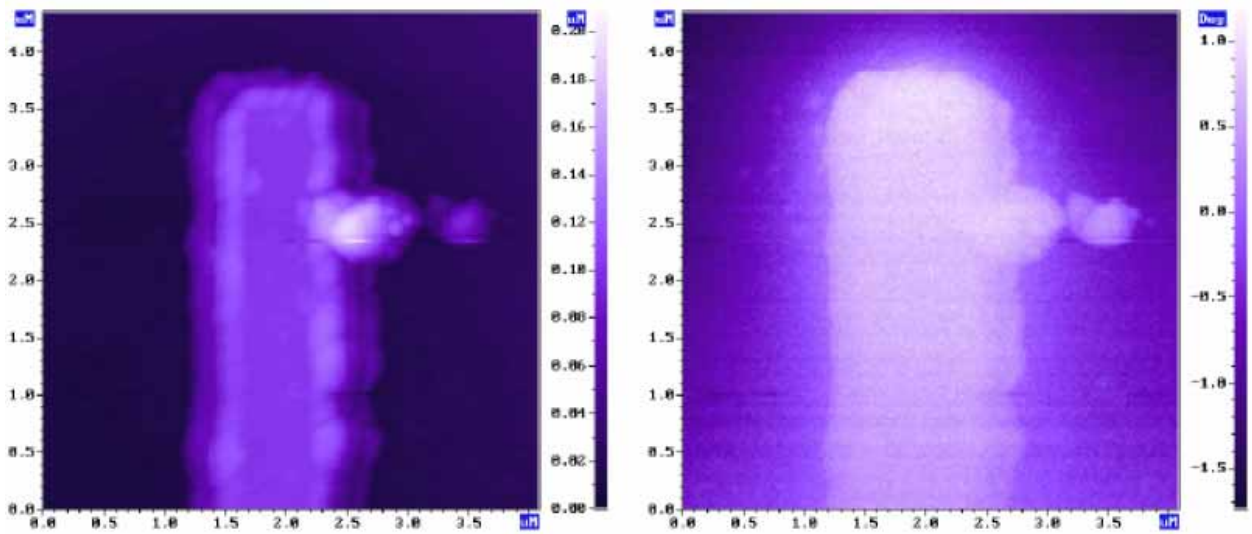

Tip-Surface Electrostatic Forces: Conductive Surface

$$F = 1/2\,(\Delta V)^2\,\partial C(z)/\partial z$$

$$\Delta V = V_{tip} - V_{surf}$$

C(*z*): tip-surface capacitance

$$C(z) = C_{apex}(z) + C_b(z) + C_c(z)$$

1. The exact functional form of **C(*z*)** is complicated and can be obtained only by numerical methods, such as finite element analysis.
2. $C_{apex}(z)$ term is considered for small tip-surface separations (***z*** << radius of curvature of tip apex).
3. For larger tip-surface separations, the contribution from the conical part of the tip $C_b(z)$ is significant.
4. The cantilever contribution $C_c(z)$ is nonnegligible at large tip-surface separations, because of the large effective area of the cantilever. $C_c(z)$ can usually be approximated as constant because the cantilever-surface separation (~10 μm) is much larger than tip-surface separation (1 to 500 nm).

Conical field emitters

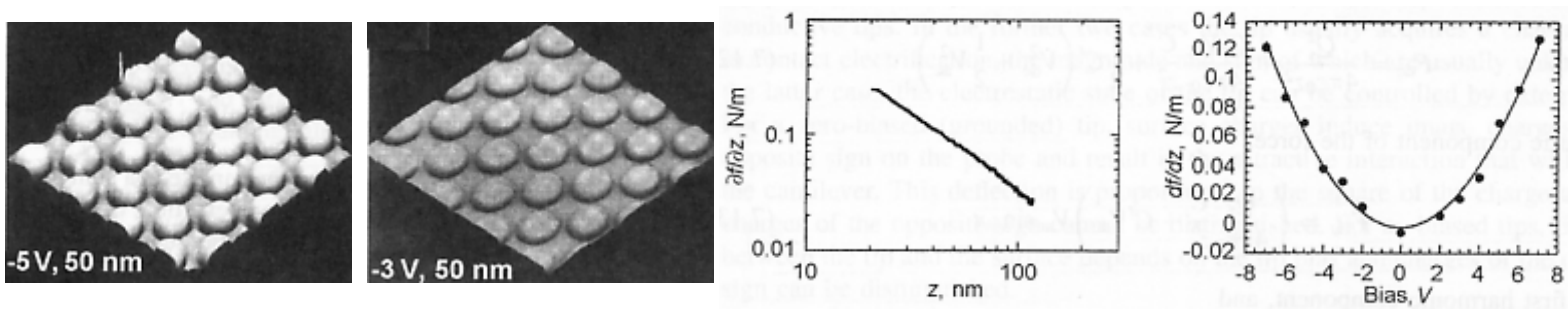

Force versus Distance for 1 V applied

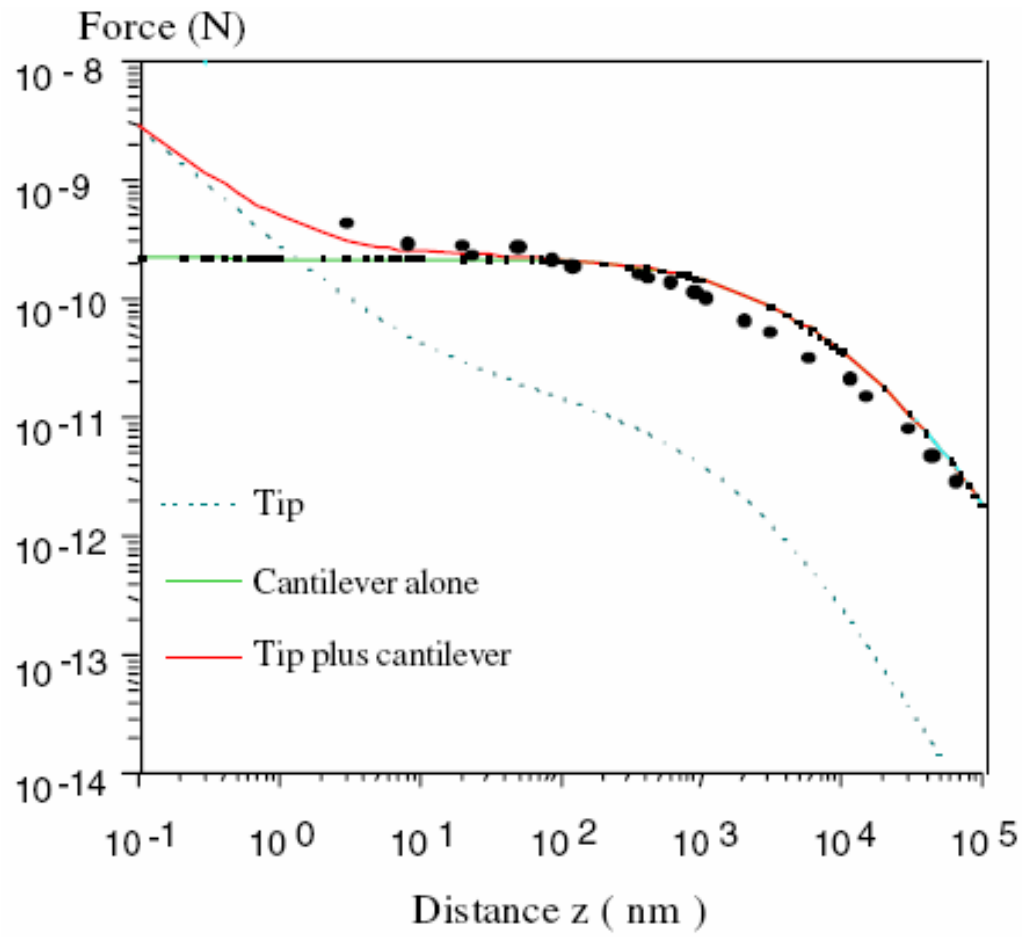

Nanotechnology **12**, 485 (2001)

Tip-Surface Electrostatic Forces: Dielectric Materials

Quantification of the electrostatic tip-surface interaction is significantly more complicated for dielectric materials, because both surface charges and volume trapped charges, as well as the tip-induced polarization image charges contribute to the total force.

$$F = \frac{Q_s Q_t}{4\pi\varepsilon_0 z^2} + \frac{1}{2} C' (V_{ac} \sin(\omega t) + V_{dc})^2 \qquad V_{tip} = V_{dc} + V_{ac}\sin(\omega t)$$

Q_s : surface charge on the sample

$Q_t = Q'_s + Q_{dc} + Q_{ac}$: charge on the tip

Q'_s image charge on the tip $\qquad Q_{dc} = V_{dc} C \qquad Q_{ac} = C V_{ac} \sin \omega t$

$Q'_s \approx -Q_s$ For localized charge $z << R$, R is the apex radius of curvature

$$F = F_{dc} + F_{1\omega} + F_{2\omega}$$

$$F_{dc} = \frac{Q_s^2}{4\pi\varepsilon_0 z^2} + \frac{Q_s V_{dc}}{4\pi\varepsilon_0} \frac{C}{z^2} + \frac{1}{2} C' \left(V_{dc}^2 + \frac{1}{2} V_{ac}^2 \right)$$

$$F_{1\omega} = \left(\frac{Q_s}{4\pi\varepsilon_0} \frac{C}{z^2} + C' V_{dc} \right) V_{ac} \sin \omega t$$

$$F_{2\omega} = -\frac{1}{4} C' V_{ac}^2 \cos 2\omega t$$

1. Measurements can be performed with dielectric, semiconductive, or conductive tips. In the former cases, the tip usually acquires a charge owing to contact electrification, the magnitude and sign of which are usually unknown. In the latter case, the electrostatic state of the tip can be controlled by external bias.

2. For a zero-biased (grounded) tip, surface charges induce image charges of the opposite sign on the probe and result in the attractive interaction, but charges of the opposite sign cannot be distinguished. For a biased tip, the force between the tip and the surface depends on the tip bias and charges of the opposite sign can be distinguished.

3. The feedback scheme that relies on the force gradient to maintain tip-surface separation may lead to tip crash into the surface in the vicinity of domain walls with opposite surface charges. This drawback is now avoided by using the non-contact scheme (Lift-Mode).

Scanning Surface Potential Microscopy (SSPM)
Kelvin Probe Microscopy(KPM)

As in EFM, this technique is usually implemented in the non-contact mode. In the second scan, the piezo is disenganged and oscillating is applied to the tip.

$$F(z) = \frac{1}{2}\frac{\partial C(z)}{\partial z}\left[(V_{dc} - V_{surf})^2 + \frac{1}{2}V_{ac}^2[1 - \cos(2\omega t)] + 2(V_{dc} - V_{surf})V_{ac}\sin(\omega t)\right]$$

$$F_{dc}(z) = \frac{1}{2}\frac{\partial C(z)}{\partial z}\left[(V_{dc} - V_{surf})^2 + \frac{1}{2}V_{ac}^2\right]$$

$$V_{tip} = V_{dc} + V_{ac}\sin(\omega t)$$

$$F_{1\omega}(z) = \frac{\partial C(z)}{\partial z}(V_{dc} - V_{surf})V_{ac}\sin(\omega t)$$

$$F_{2\omega}(z) = \frac{1}{4}\frac{\partial C(z)}{\partial z}V_{ac}^2\cos(2\omega t)$$

1. The lock-in technique allows extraction of the first harmonic signal, $F_{1\omega}$. A feedback loop is employed to keep it equal to zero (nulling force approach) by adjusting V_{dc} on the tip. When $V_{dc} = V_{surf}$, $F_{1\omega} = 0$. Thus the surface potential is measured.
2. The high spatial and voltage resolution (~ mV) make KPM a prominent tool for the characterization of current devices, especially intergated circuit analysis..
3. This technique is also sensitive to local charge on the surface.

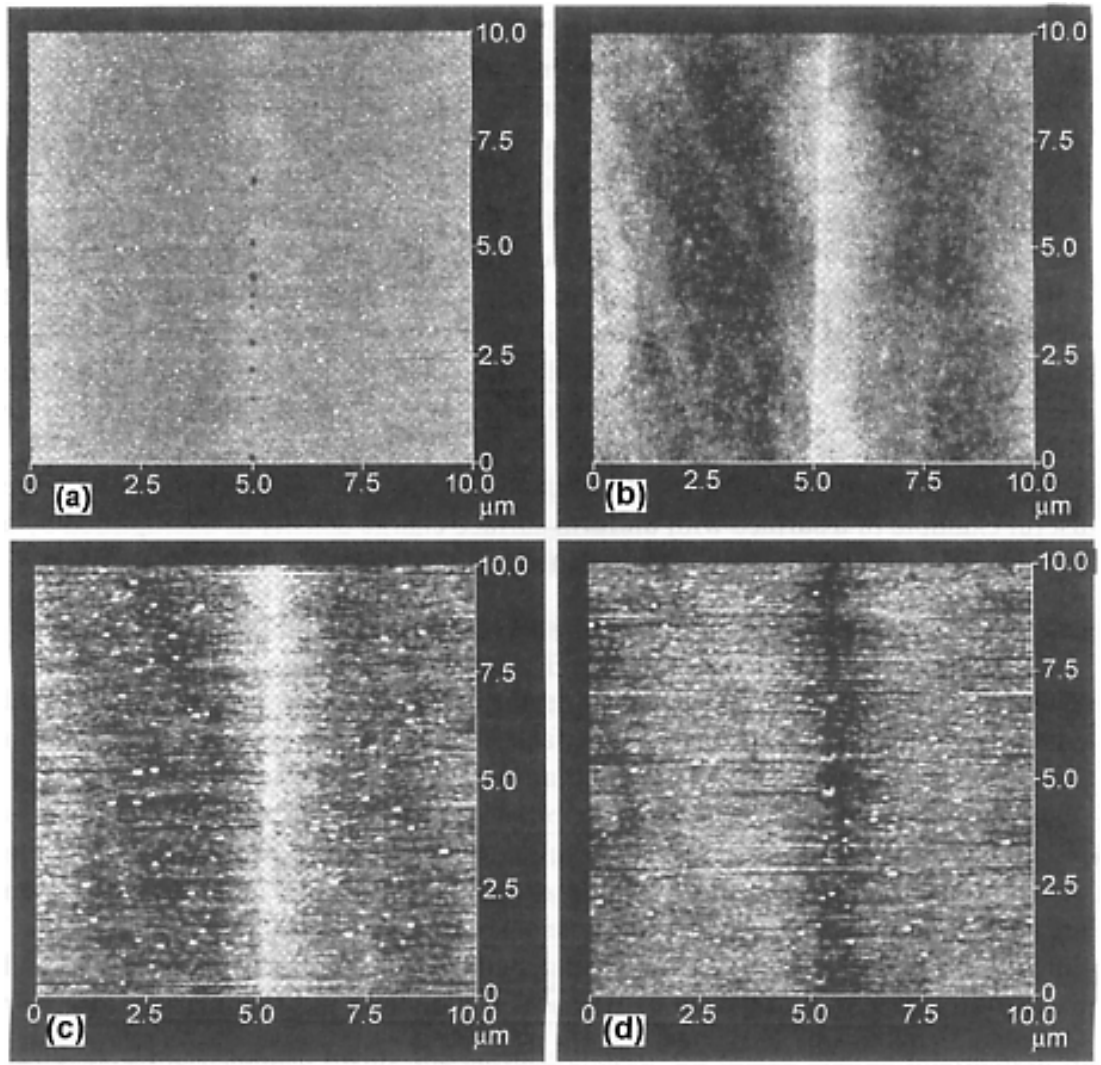

Figure 7.2. **a**, Topography of Nb-doped 36.8° $SrTiO_3$ bicrystal in the vicinity of grain boundary (**a**). **b**, Surface potential (SSPM) image of the same region. **c**, EFM (force gradient) images at tip bias $V_{tip} = 5V$ and (**d**) $V_{tip} = -5V$. The range is (**a**) 5 nm, (**b**) 20 mV and (**c**, **d**) 2 Hz.

Simple interpretation of KPM in terms of surface potential is applicable only for conductive surfaces. Even though KPM has been successfully applied to the characterization of semiconductor and dielectric surfaces, the image formation mechanism is not yet clearly understood. Such factors as tip-induced band-bending, charge injection, a contact electrification, and redistribution of surface adsorbates all can contribute to the observed potential image, rendering its interpretation and quantification complicated tasks. Nevertheless, sensitivity of KPM to the local variations of work function and Fermi level allows its application to dopant profiling in semiconductor devices.

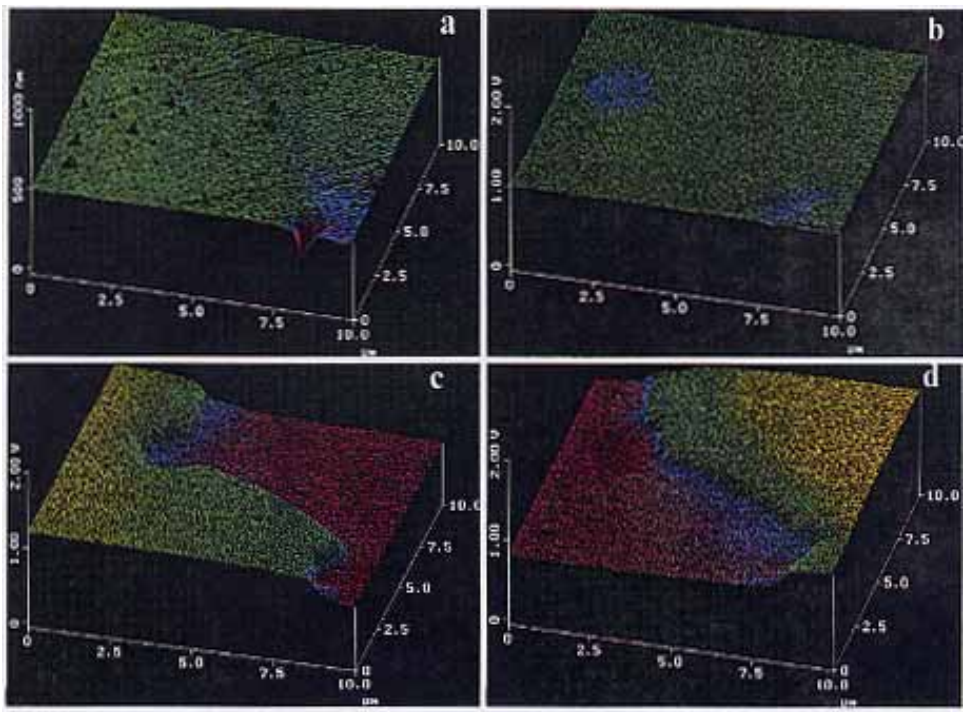

Figure 7.5. Polycrystalline ZnO. **a**, Topographic structure in an AFM image. **b**, Surface potential image identifying secondary phases with a 100 mV difference at the surface. Surface potential with (**c**) negative and (**d**) positive lateral voltage applied on the sample showing a 0.3 V potential drop at the grain boundary. (Reprinted with permission from Ref. 36.)

ZnO

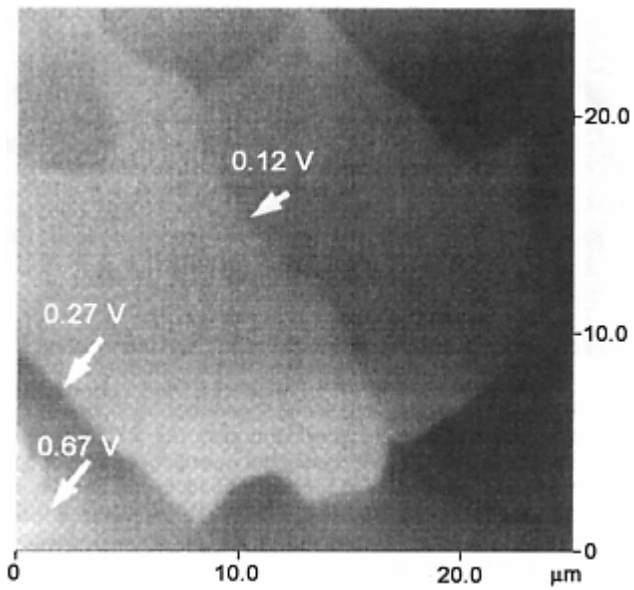

Nanotechnology **12**, 485 (2001)

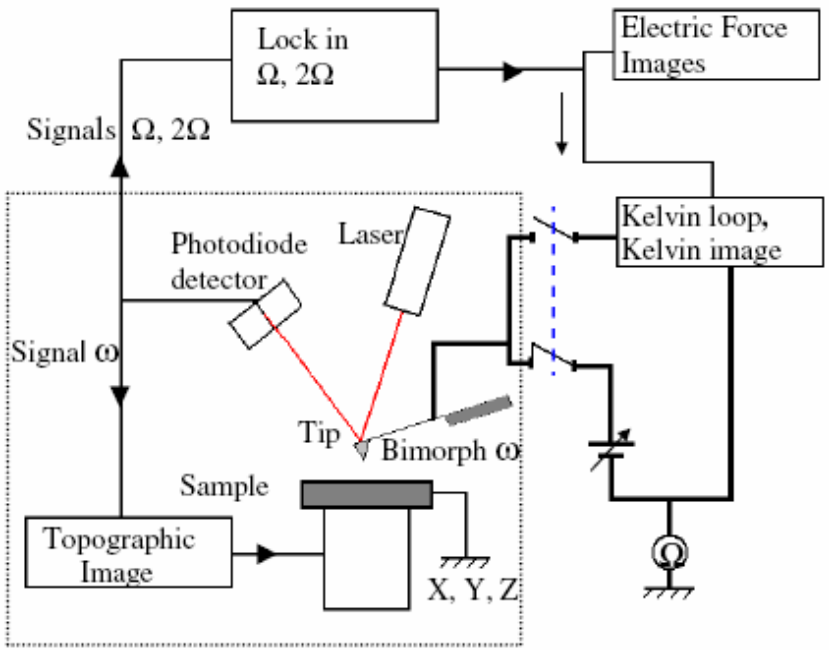

Semiconductor Laser

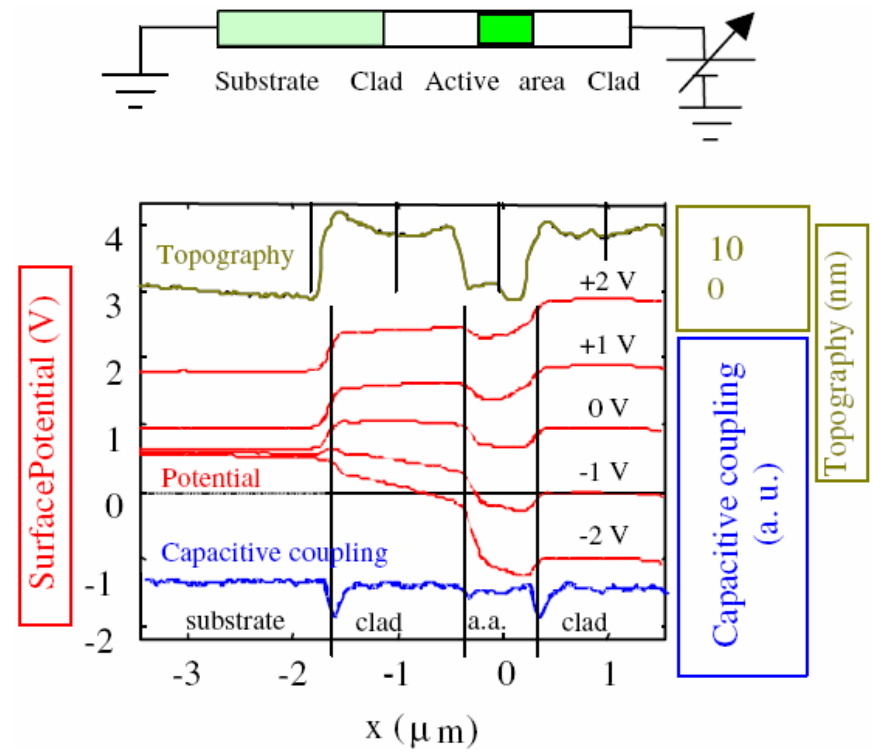

InAs/GaAs Nanoislands

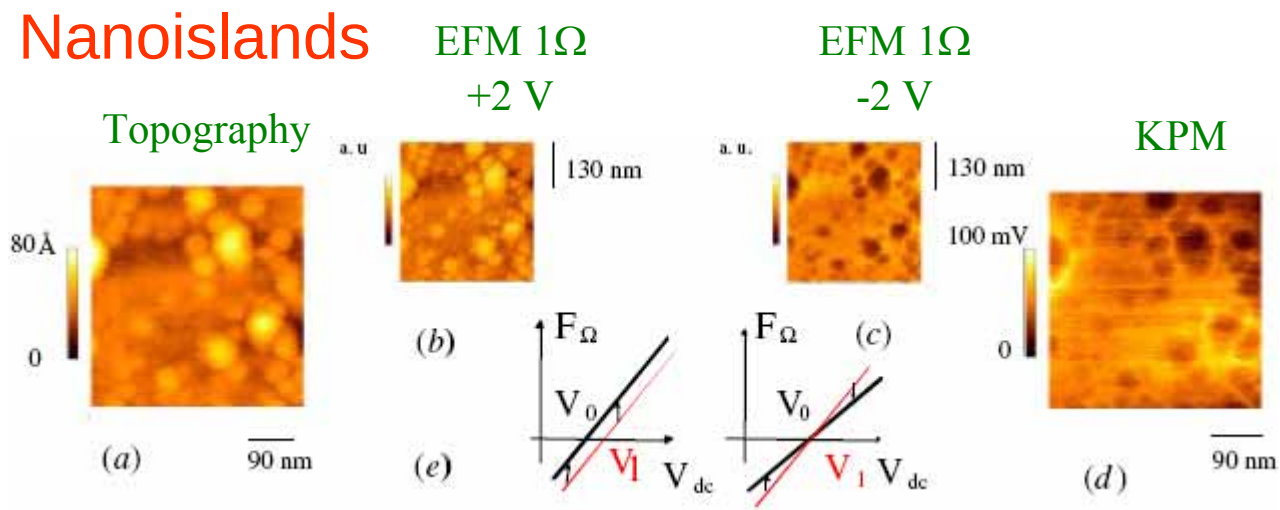

Case Study

EFM is a useful failure analysis tool on the device, wafer, or chip level - even on packaged IC's.

a live packaged SRAM IC with passivation layer on

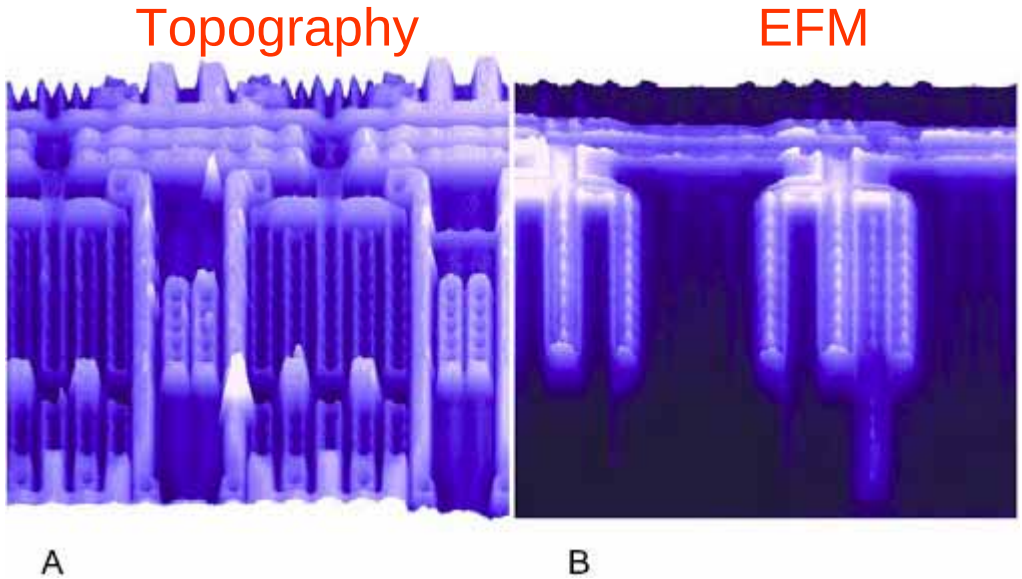

80μm

1. The electric signal between the second and third prongs from the left shows that the transistor on the left is in saturation. The topography image shows no hint of this failure.
2. Using emission microscopy first, a defect was detected in the vicinity of this transistor, but the cause and the exact location of the defect were not identifiable until the EFM image was captured. With the passivation removed, and then reactive ion etch strip-back to the gate oxide, AFM topography images of another defective transistor very close to this area revealed an ESD (electrostatic discharge)-induced rupture hole in the gate oxide of that transistor (not shown).

Case Study

1. InP-based nanowire between two metal contacts with a bias applied.

Topography KPM

Electrical transport measurements

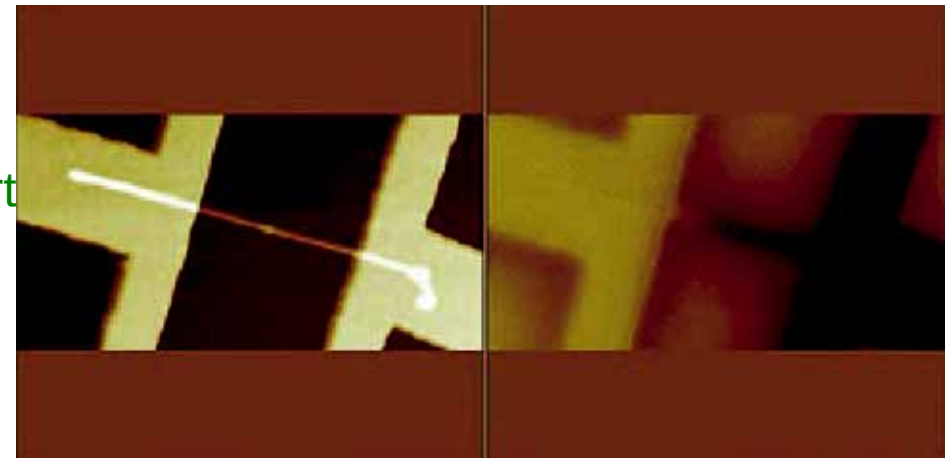

2µm x 1µm

Potential maps can be used to identify bottlenecks to charge transport and, in conjunction with simultaneous drain current measurements, allow resistance analysis of specific structures, e.g., contacts and discontinuities in the channel.

2. Pentacene TFT

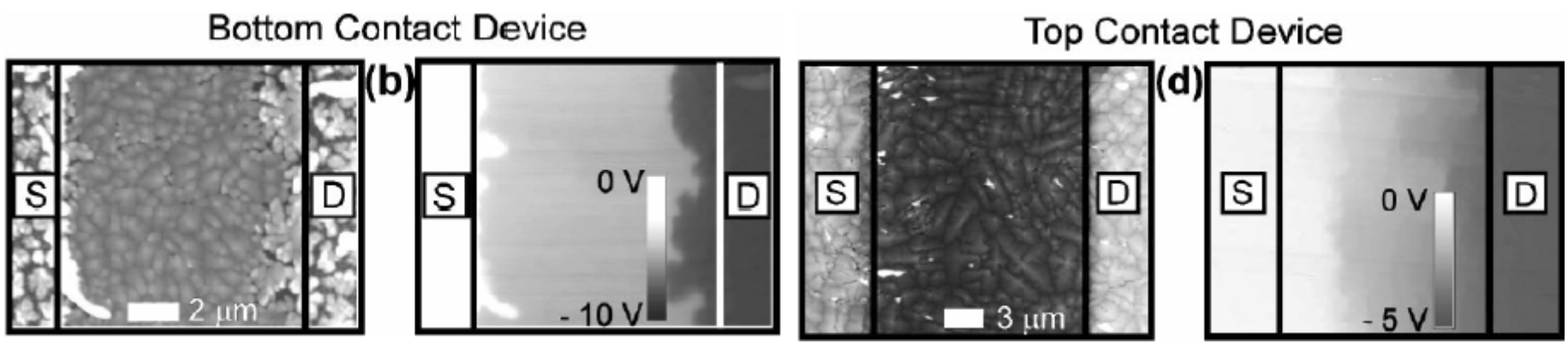

Topography Surface potential

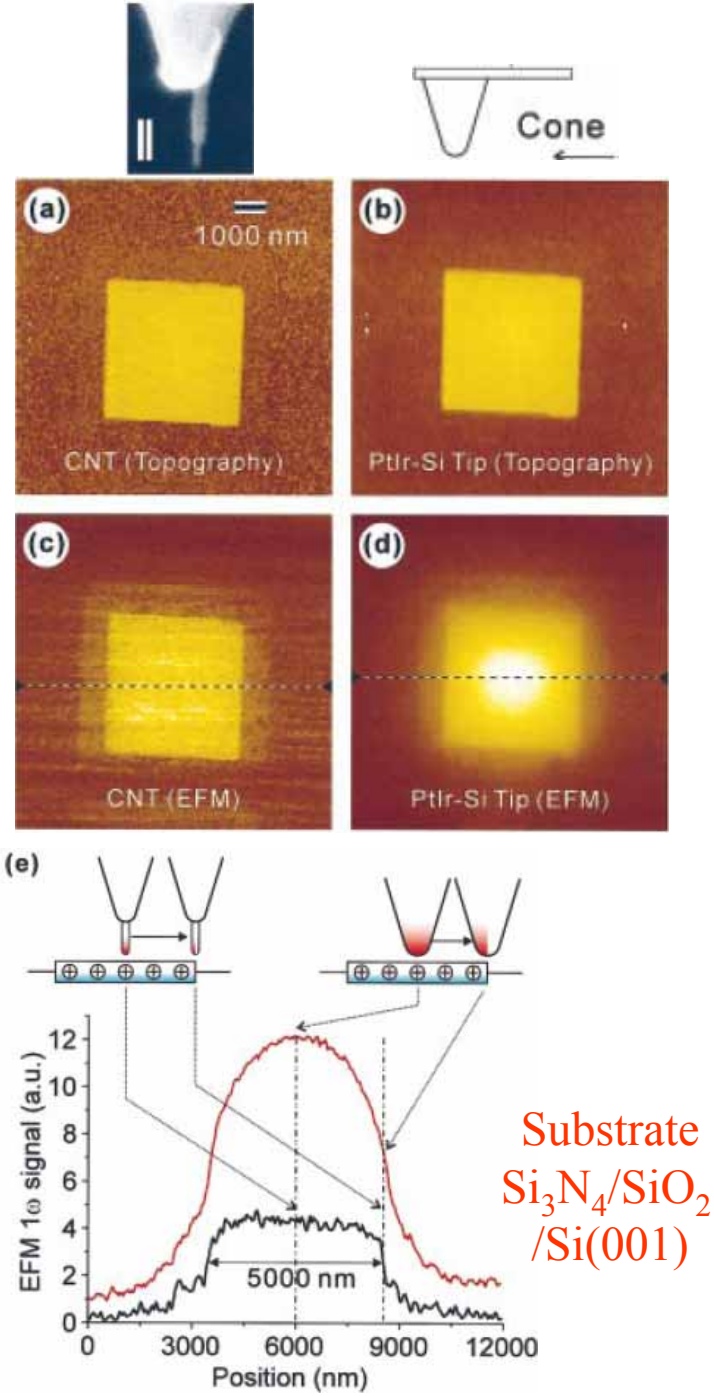

Substrate
Si_3N_4/SiO_2
/Si(001)

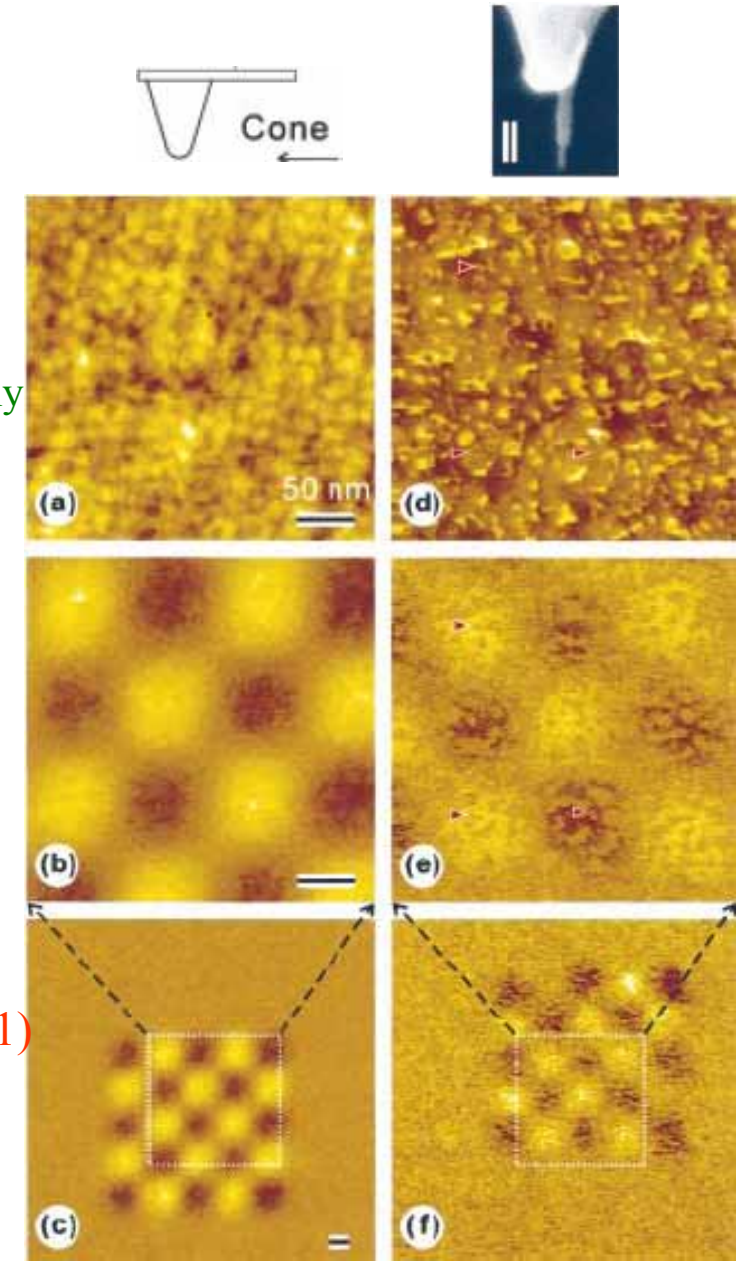

Gwo, Appl. Phys. Lett. 26, 5042(2002).

Precision Control of the Number and Position of Dopant Atoms

As the size of semiconductor devices continues to shrink, the normally random distribution of the individual dopant atoms within the semiconductor becomes a critical factor in determining device performance—homogeneity can no longer be assumed.

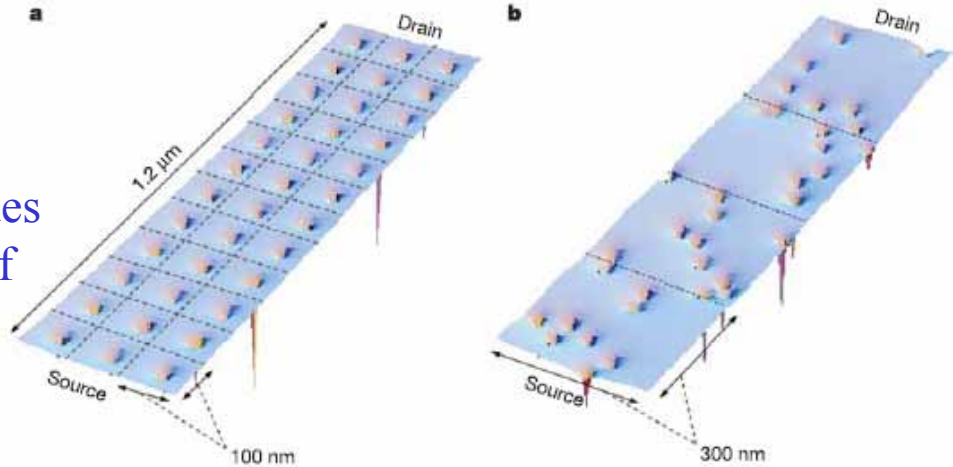

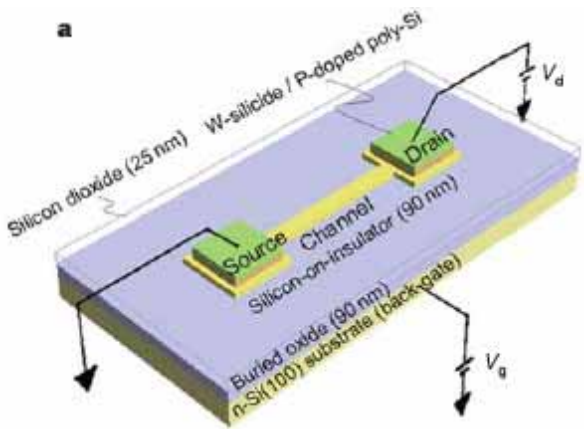

AFM

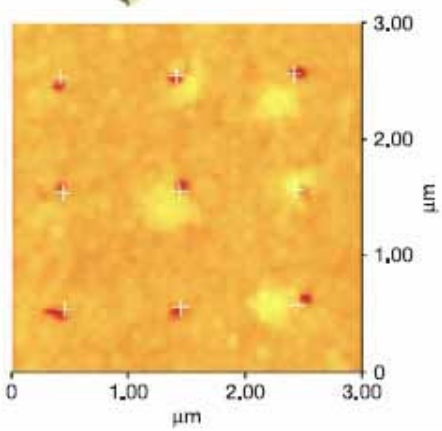

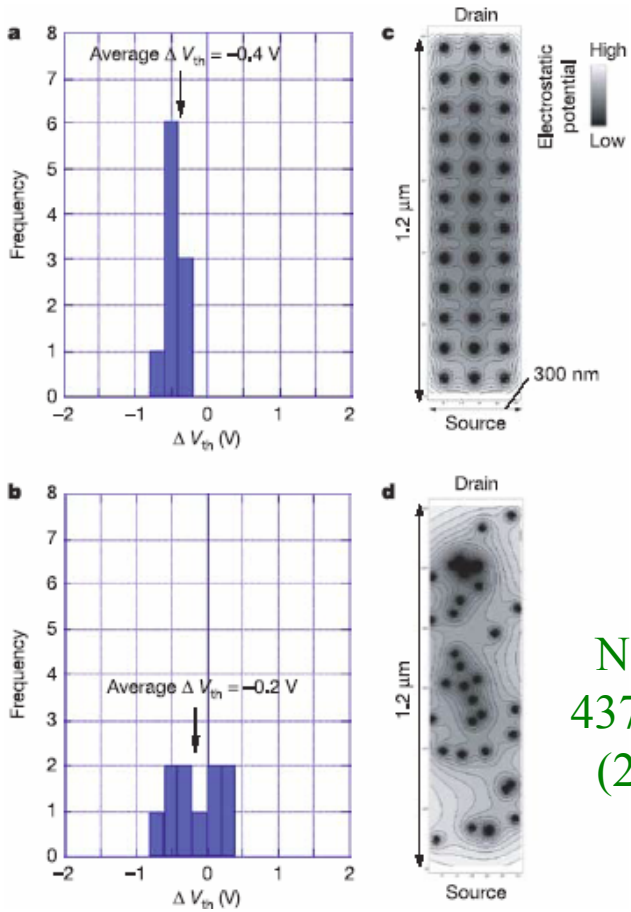

Nature 437,1128 (2005)

Scanning Capacitance Microscopy (SCM)

1. With the continuous shrinking of device dimension, there is an increasing demand for measuring doping profile with high spatial resolution. Scanning capacitance microscopy (SCM) has proven to be a quick and convenient method for direct imaging of submicron devices and a promising technique for two dimensional dopant profiling.

2. Traditional Scanning Electron Microscope (SEM) imaging has difficulty distinguishing between wells and substrates, particularly in the case of similarly doped wells and substrates, such as a P well in a P type wafer. The SCM can image doping concentrations allowing the user to view features.

3. The fundamental principle of SCM is based on the metal-oxide-semiconductor concept. The tip of the AFM cantilever acts as the metal and a layer of insulating oxide is grown on top of the semiconductor sample. The tip-sample capacitance can be probed by modulating carriers with a bias containing ac and dc component. The magnitude of the SCM output (dC/dV) signal is a function of carrier concentration.

SCM CV Curve

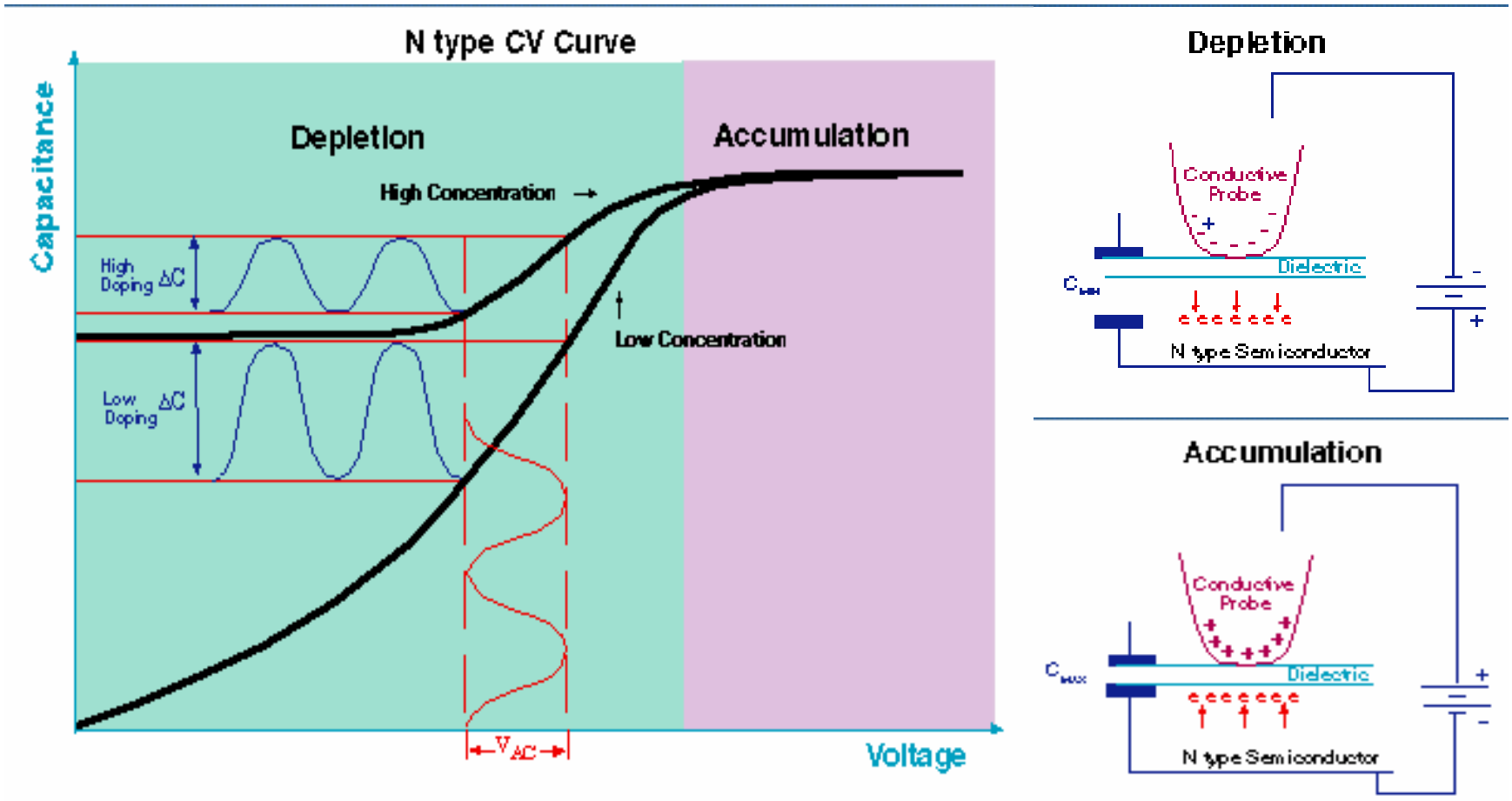
N type CV Curve
Capacitance
Depletion
Accumulation
High Concentration
Low Concentration
High Doping ΔC
Low Doping ΔC
V_{AC}
Voltage
Depletion
Conductive Probe
Dielectric
C_{min}
N type Semiconductor
Accumulation
Conductive Probe
Dielectric
C_{max}
N type Semiconductor

掃描電容顯微術(SCM)

Operational principle of the SCM

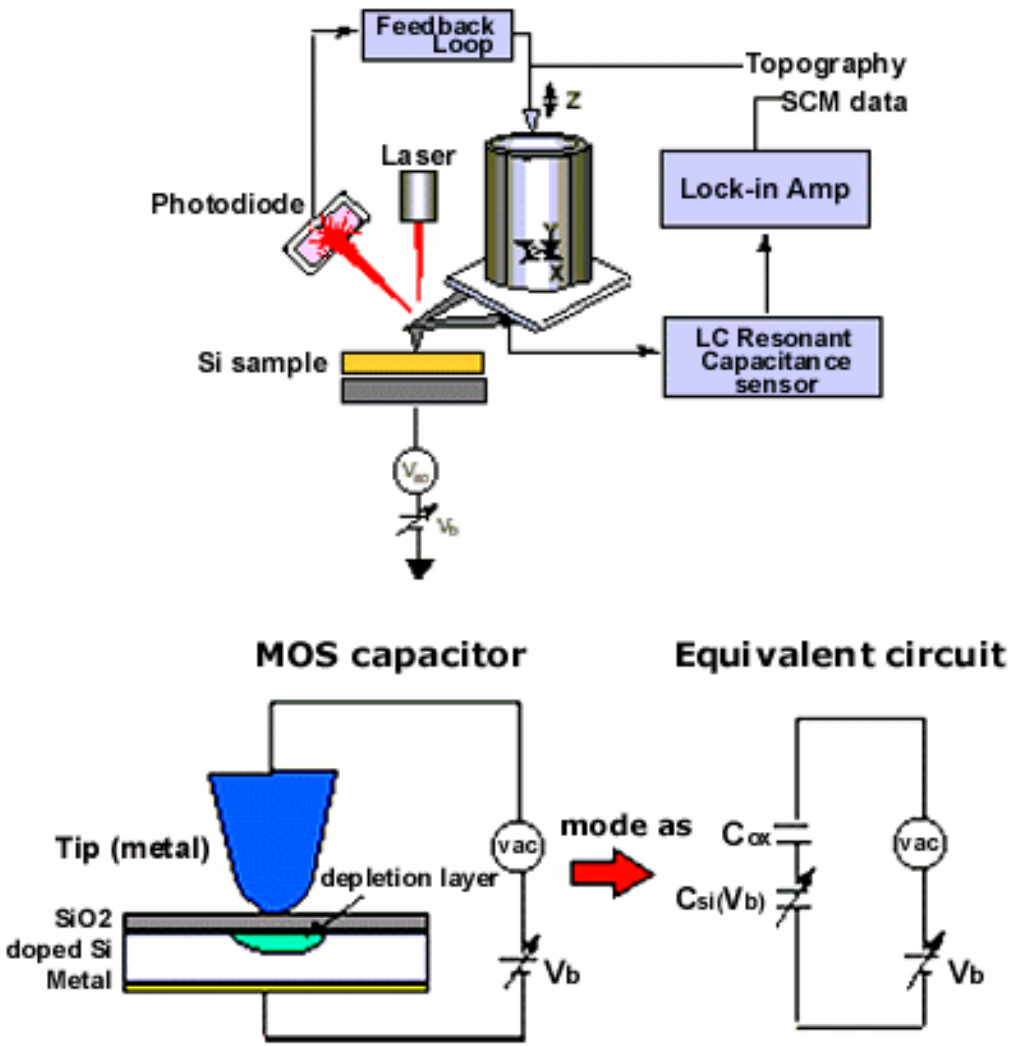

SCM imaging requires the sample surface to be low roughness (<0.1nm), no surface damage, and clean. Back ohmic contact is needed.

1. **Most SCMs are based on contact-mode AFM with a conducting tip.**
2. **In SCM, the sample (or the metallic tip) is covered with a thin dielectric layer, such that the tip-sample contact forms a MIS capacitor, whose C-V behavior is determined by the local carrier concentration of the semiconductor sample.**
3. **By monitoring the capacitance variations as the probe scans across the sample surface, one can measure a 2D carrier concentration profile.**
4. **One usually measures the capacitance variations (dC/dV), not the absolute capacitance values.**
5. **No signal is measured if the probe is positioned over a dielectric or metallic region since these regions cannot be depleted.**

References:

1. C.C. Williams, Annu. Rev. Mater. Sci. **29**, 471 (1999).
2. P.D. Wolf et al., J. Vac. Sci. Technol. B **18**, 361 (2000).
3. R.N. Kleiman et al., J. Vac. Sci. Technol. B **18**, 2034 (2000).
4. H. Edwards, et al., J. Appl. Phys. **87**, 1485 (2000).
5. J. Isenbart et al., Appl. Phys. A **72**, S243 (2001).

Scanning Capacitance Microscopy

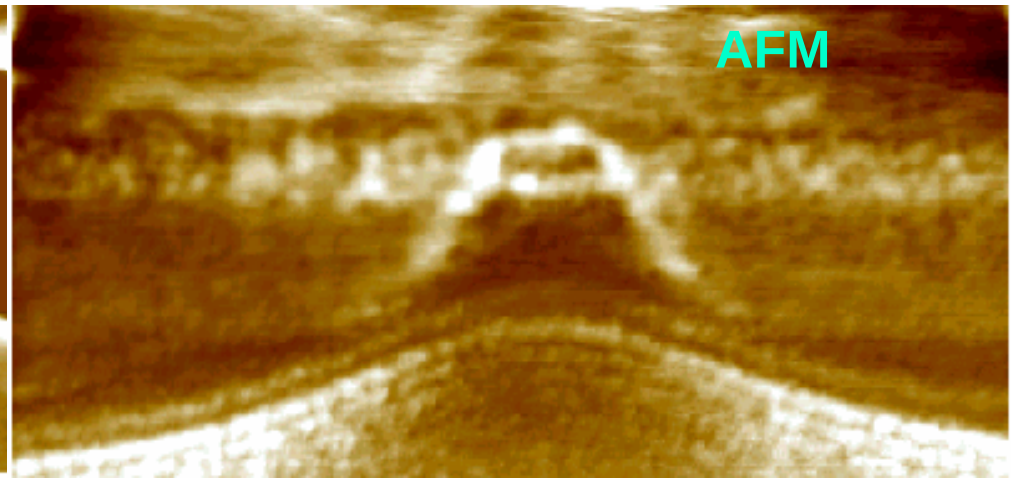

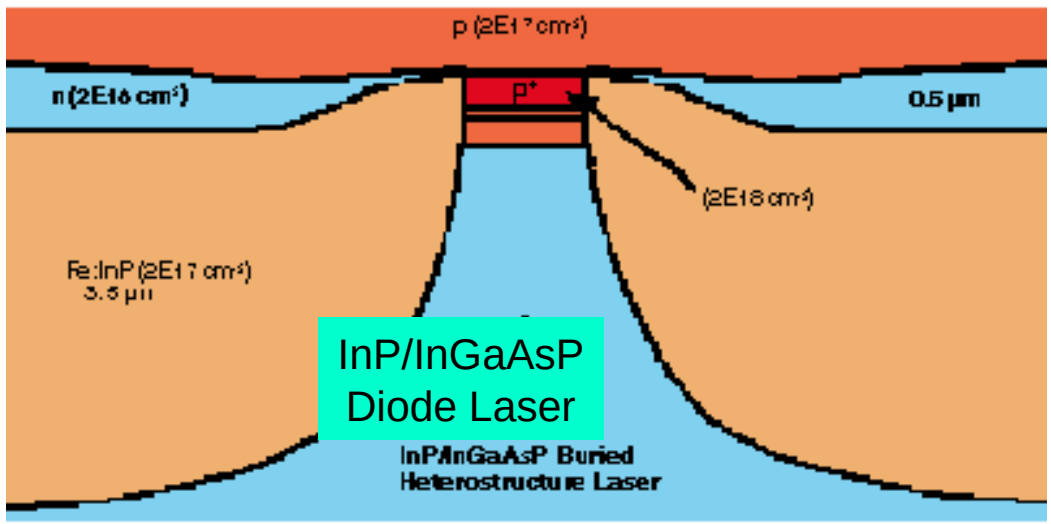

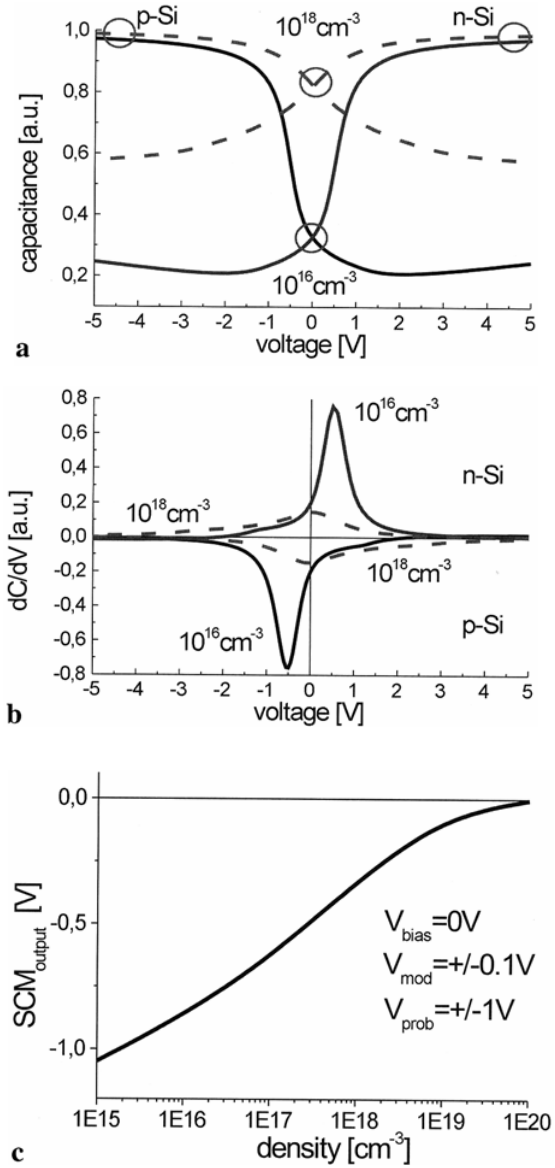

Fig. 2a–c. 3D simulations of SCM on homogeneously doped samples. The tip ($r_a = 25$ nm, $r_i = 25$ nm, $\alpha = 20°$) is modelled in cylindrical coordinates; $d_{Ox} = 10$ nm. **a** $C(V)$ curves on p- and n-doped silicon with dopant concentrations of 10^{16} cm^{-3} and 10^{18} cm^{-3}, respectively. **b** The corresponding $dC/dV(V)$ curves are calculated analytically. **c** The calibration curve is calculated from $C(V)$-curve simulations. The SCM output is calculated as $\Delta C/\Delta V(V)$ at $V_{bias} = 0$ V taking $V_{mod} = \pm 0.1$ V and $V_{prob} = \pm 1$ V into account

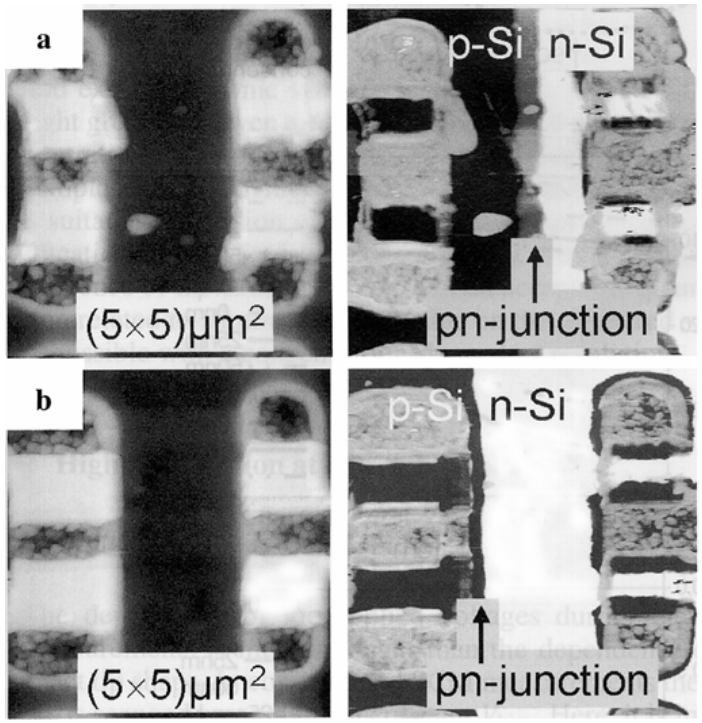

Fig. 3a,b. Failure analysis of an industrial device by means of SCM. Topography (*left-hand side*) and SCM image (*right-hand side*) are taken simultaneously. **a** Well-operating device with the *pn* junction implanted in the middle between the poly-silicon contacts. **b** Defective device with the *pn* junction shifted to the left-hand contacts. Both devices were measured at the same V_{bias} corresponding to the "zero voltage" (see text)

J. Isenbart et al., Appl. Phys. A **72**, S243 (2001).

Influence of V_{bias} on the position of a p-n junction

Lateral Resolution

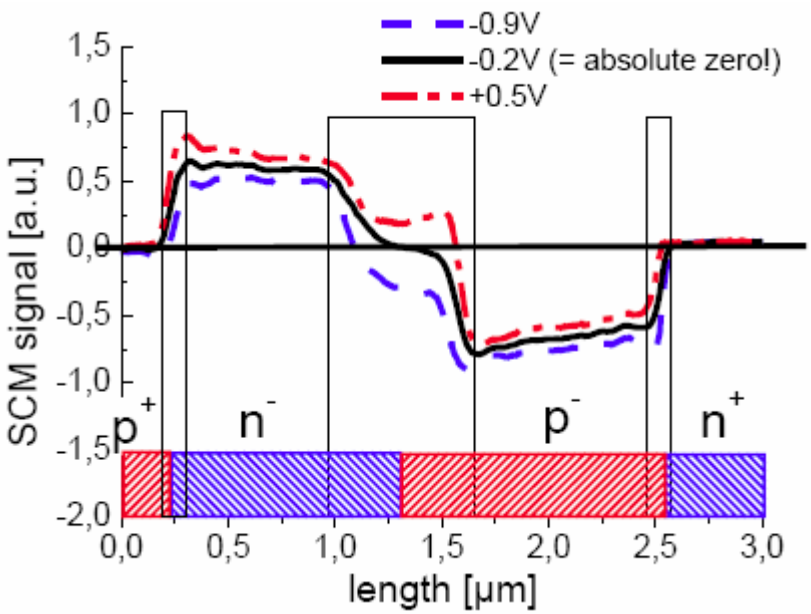

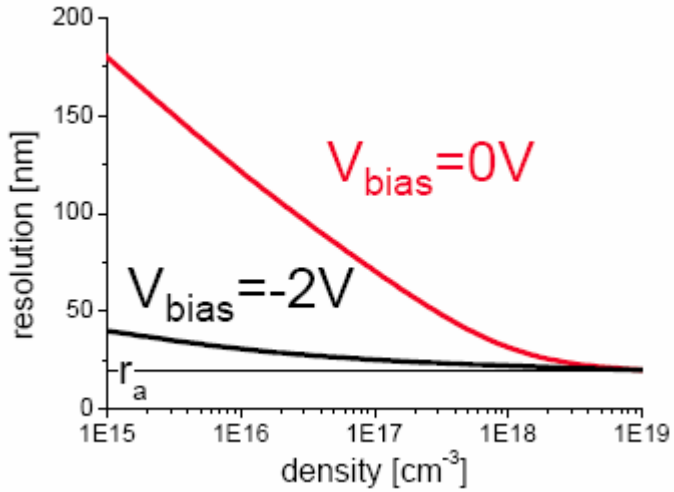

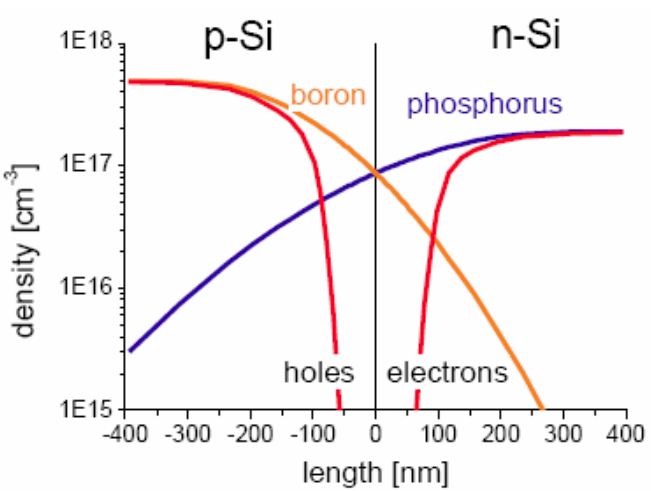

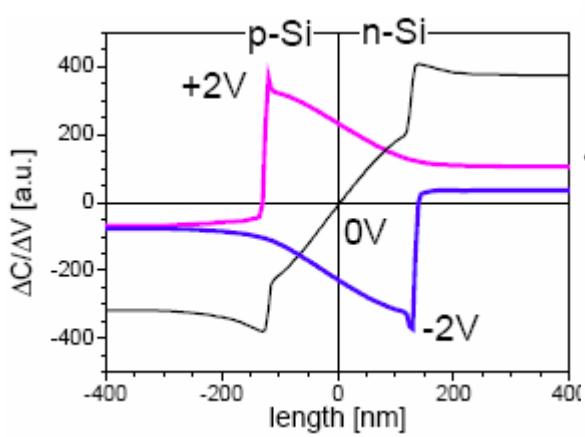

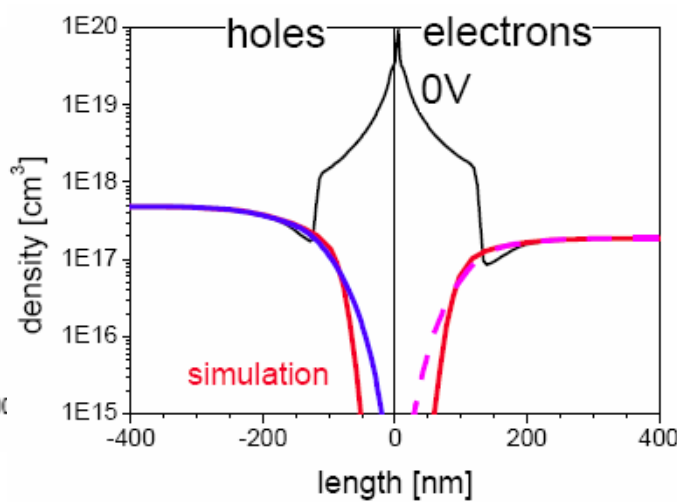

Differential Capacitance (open loop) mode, ΔC mode

Topography dC/dV

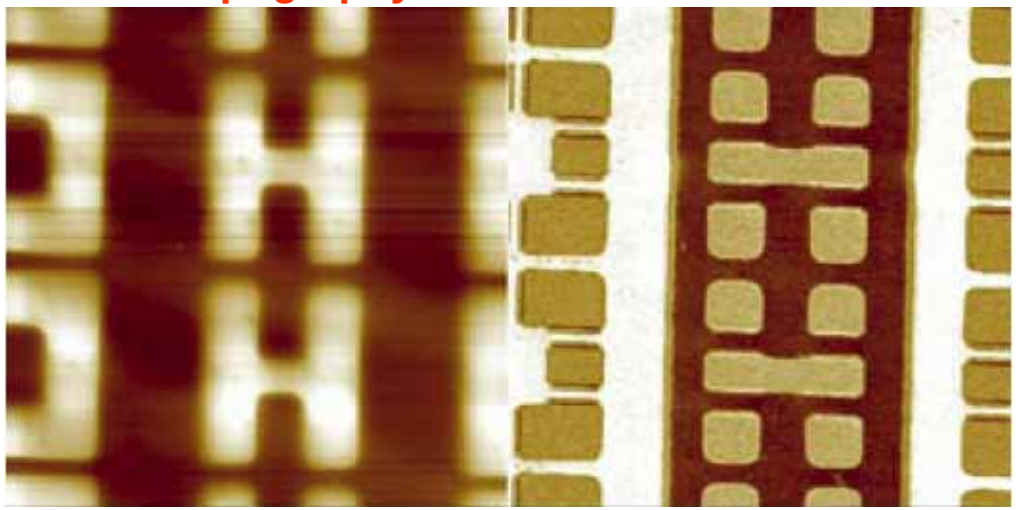

Open loop imaging, n and p type material exhibit different polarity.

In the ΔC mode, the response of the charge carriers is greatest in the lightly doped area. In highly doped area, n+ and p+ will appear slightly brighter and slightly darker than insulating area. When the tip is over a lightly doped region, the spatial resolution is degraded, because it leads to a large depletion depth and a larger change in capacitance. The ΔV mode can overcome the limitation, because the depletion width is kept constant

Differential Voltage (close loop) mode, ΔV mode

Topography ΔV

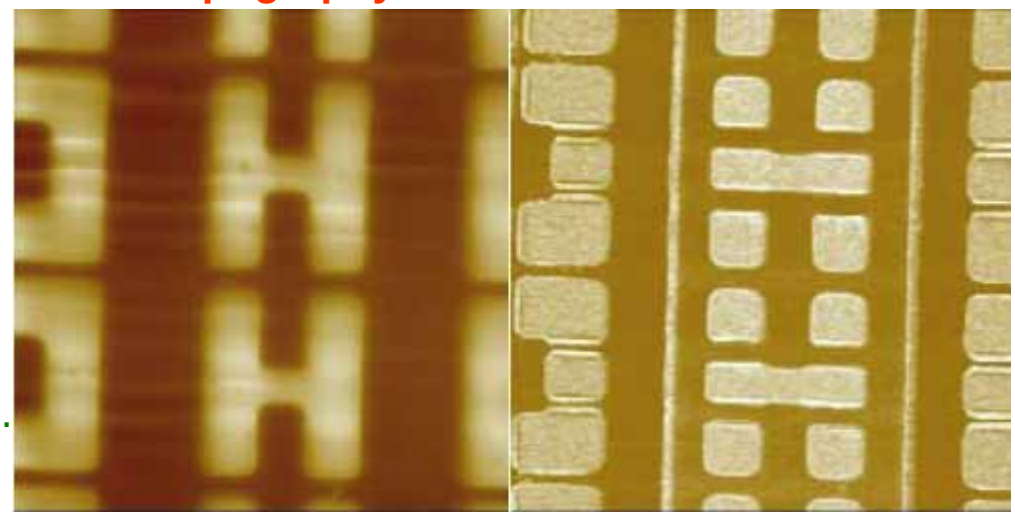

High signal indicates highly doped area; low signal indicates lightly doped area.

The magnitude of the ac bias voltage applied to the sample is adjusted by a feedback loop to maintain a constant capacitance change. The feedback controlled ac bias voltage is measured.

Case Study

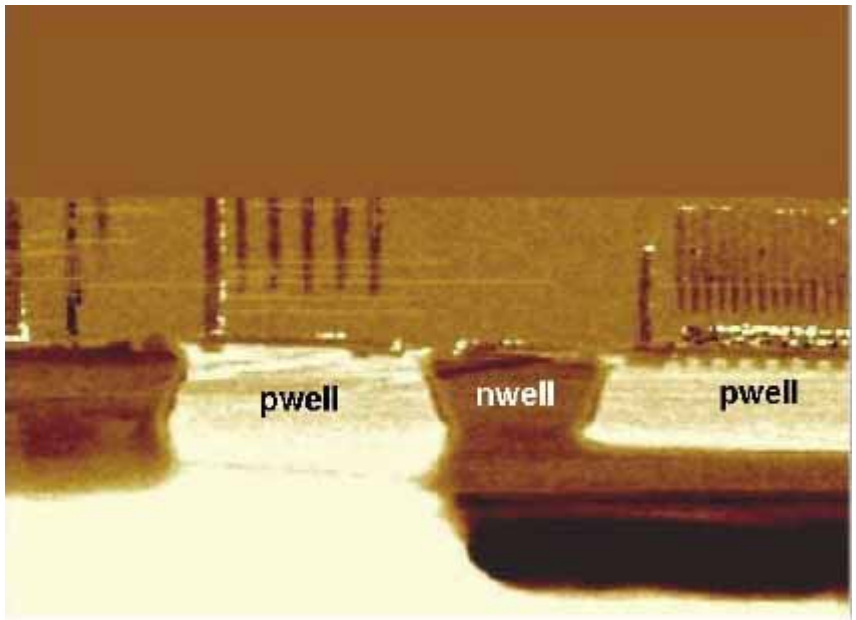

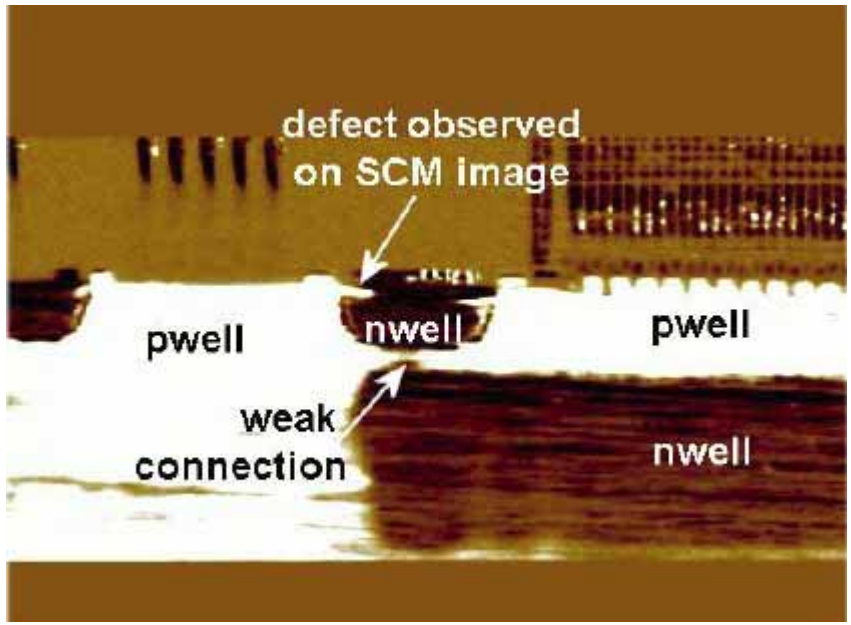

SCM image of a good location. Note the good connection between the n-well and deep n-well beneath it.

SCM image of the failing sample revealing the defects in the n-well.

Scanning capacitance microscopy (SCM) is increasingly valuable for failure analysis.

1. The SCM has proven its potential for the analysis of 2D dopant profiles on a scale down to less than 50 nm.
2. The quantification of a measured dopant profile is still difficult due to the influence of parameters of the sample, the tip shape, and the capacitance sensor including the applied voltages.
3. The properties of the sample, e.g. the roughness of the surface (fluctuation of the oxide thickness), the density of charged impurities and traps in the oxide layer and mobile surface charges, are mainly determined by the sample-preparation procedure.
4. The most important influence on the measurements is due to the probing voltage of the capacitance sensor and the applied bias voltage.
5. In SCM, not the dopant concentration, but rather the local charge-carrier concentration is measured because only the mobile carriers can contribute to C(V) and thus only the local charge-carrier distribution can be detected.
6. What makes the SCM significant is that it is increasingly difficult to accurately reveal semiconductor well profiles and junctions as well as measure carrier concentrations. Up to now we have been able to use lower resolution techniques such as Spreading Resistance Profiling (SRP) and Secondary Ion Mass Spectrometry (SIMS). However these are now incapable of coping with the micro-minuscule dimensions of today's state-of-the-art devices. The SCM has an ultimate resolution of less than 20 nanometers, so this is a significant enhancement to our existing analytical capabilities.

TABLE II. Summary of the different scanning probe microscopy techniques which can be used for 2D carrier profiling of semiconductor devices. The "mode" reflects the scanning mode which is being used to control the movement of the probe (NC=noncontact; C=contact).

Technique	Mode	Probe	Measured quantity
Scanning tunneling microscopy/ spectroscopy (STM/STS)	STM	Metallic needle	No. doping atoms $I-V$ spectra
Selective etching+atomic force microscopy	NC-AFM	Ultrasharp Si	Topography after chemical etch
Scanning capacitance microscopy/ spectroscopy (SCM/STS)	C-AFM	Metal-coated Si or metallic	Depletion capacitance $C-V$ spectra
Scanning spreading resistance microscopy (SSRM)	C-AFM	Diamond-coated Si or diamond	Electrical resistance $I-V$ spectra
Kelvin probe force microscopy (KPM)	NC-AFM	Metal-coated Si or metallic	Electrostatic potential (electric field)
Scanning surface harmonic microscopy (SSHM)	STM	Metallic needle with microwave cavity	Depletion capacitance

P.D. Wolf et al., J. Vac. Sci. Technol. B **18**, 361 (2000).

TABLE III. Intercomparison of two-dimensional doping (D) and carrier (C) profiling methods (NA=not available).

Method	Ref.	Resol. (nm)	Range (cm^{-3})	Conc. resol.	D/C	Quantifiable	Comments and problems
			SPM techniques				
SCM	(43–59)	10	1e15–1e20	Power	C	Limited	Uncertainties at junctions, poor quantification procedure
SSHM	(60–62)	5	NA	Power	C	No	No quantification procedure
STM-atom counting	(20–23)	Atomic	1e18–1e20	Linear	D	Yes	Only on GaAs, not on Si
STM-STS/ CITS	(24–26) (31,32)	10	NA	Log.	C	Limited	Only junction delineation and type (n or p) identification
STM-STP	(27–30)	10	NA	Limited	C	Limited	Only junction delineation
KPM	(66,67)	100	1e15–1e20	Limited	C	Limited	Poor quantification procedure, stray-fields limit the resolution
SSRM	(68–73)	20	1e15–1e20	Linear	C	Yes	Availability diamond probes
Chemical etch +AFM/STM	(37–39)	10–20	1e17–1e20	Limited	C	Limited	Difficult to quantify, poor reproducibility

Scanning Near-Field Optical Microscopy (SNOM, NSOM)

1. The lateral resolution of conventional far-field optical microscopy is fundamentally limited by diffraction to ~ $\lambda/2$, where λ is the optical wavelength.
2. The SNOM is a scanning probe microscope that allows optical imaging with spatial resolution beyond the diffraction limit. A nanoscopic light source, usually a fiber tip with an aperture smaller than 100 nm, is scanned very closed to the sample surface in the region called "optical near-field".
3. The achievable optical resolution is mainly determined by the aperture size of the optical probe and the probe-surface gap.
4. The fiber tip is held tens of nanometers above the surface, and both a topographic and optical image of the sample may be generated simultaneously. Fluorescence (UV/Visible light range) spectra may be recorded by holding the tip over a single feature.

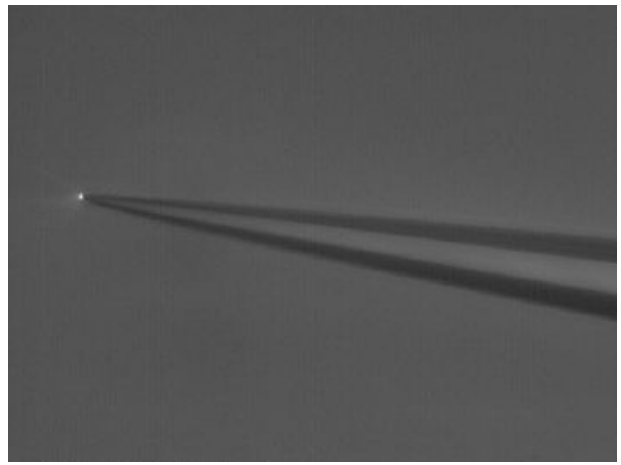

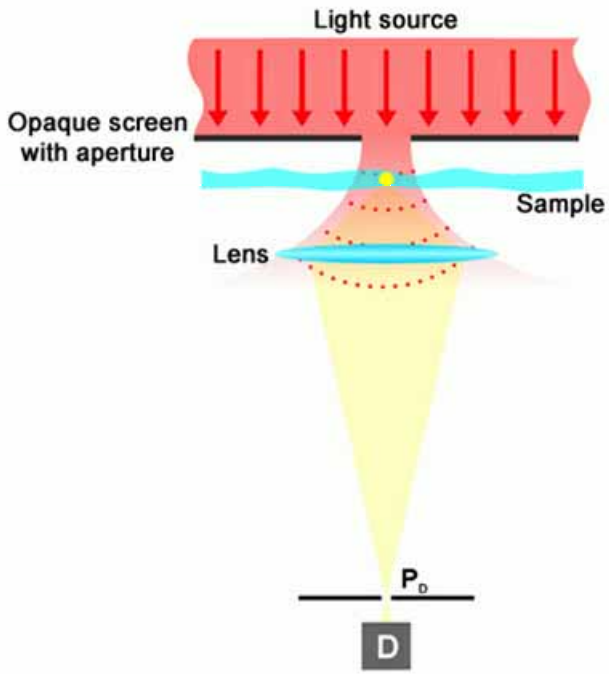

近場光學顯微術(NSOM)

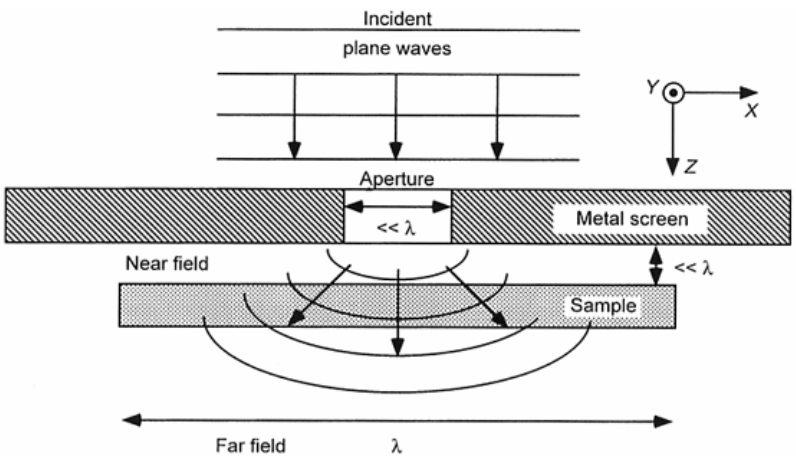

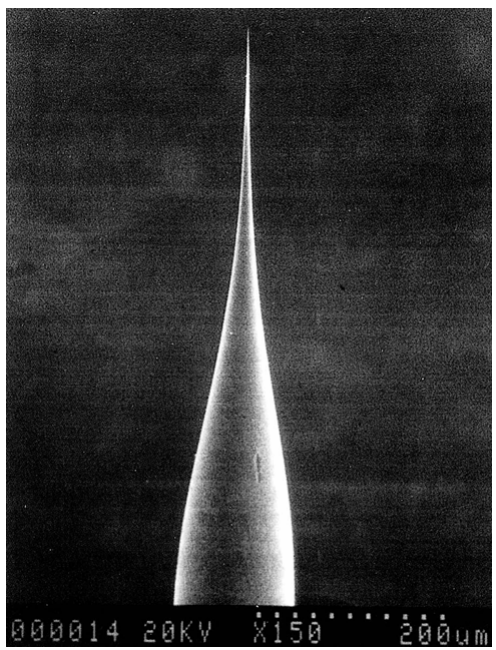

Illumination mode

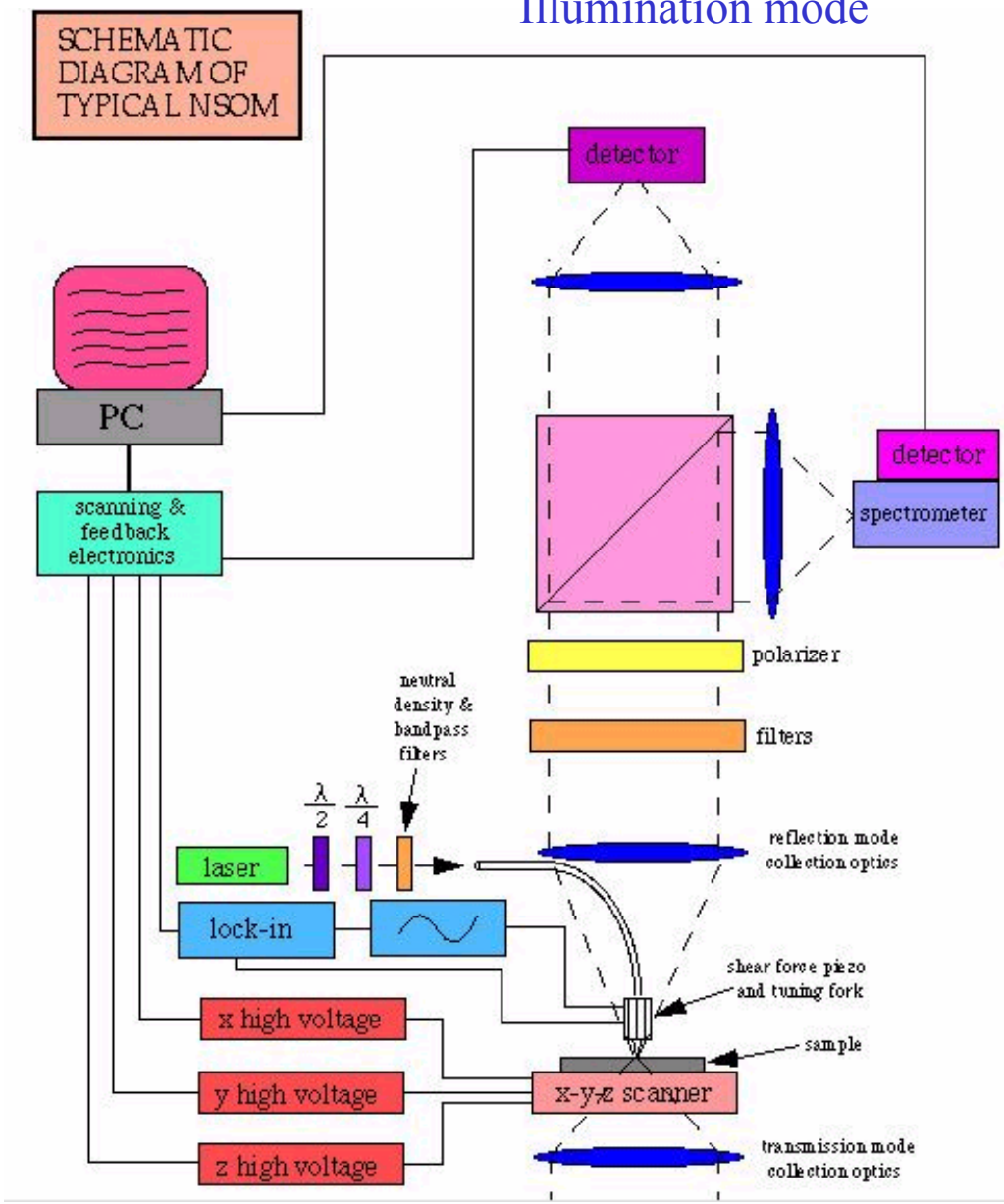

Fiber Optic Probe

1. Probe tapering: diameter of the optical aperture, optical throughput of the probe.
2. Metallic coating: When the probe diameter decreases to subwavelength dimensions, the light is no longer confined to the fiber. If no coating is employed, a majority of the light simply exits the fiber at this point.
   Al is almost always employed as the coating material in visible-light NSOM.
   Reflectivity ≈ 90% near 500 nm. Skin depth ≈ 13 nm at 500 nm.
   Ag: reflectivity ≈ 95% near 500 nm. Au: reflectivity < 70% (stronger probe heating problem).
3. Feedback methods:
   Shear-force feedback
   Tapping mode

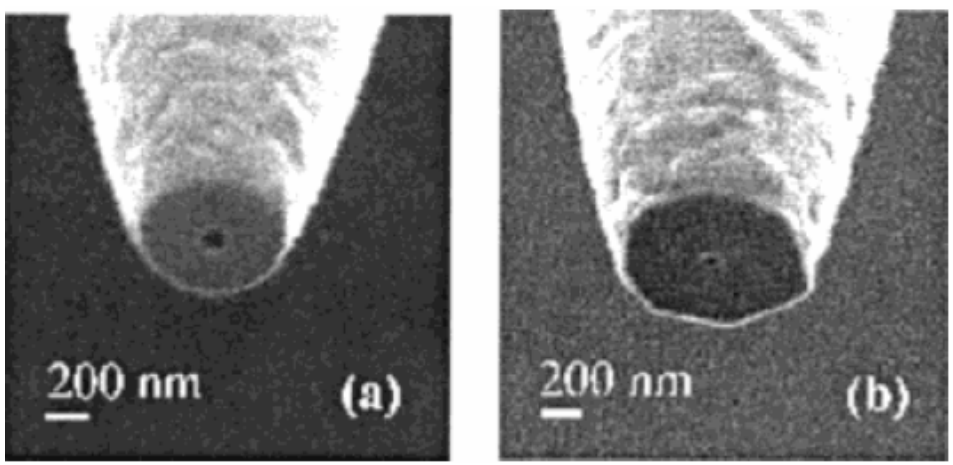

Shear-force feedback

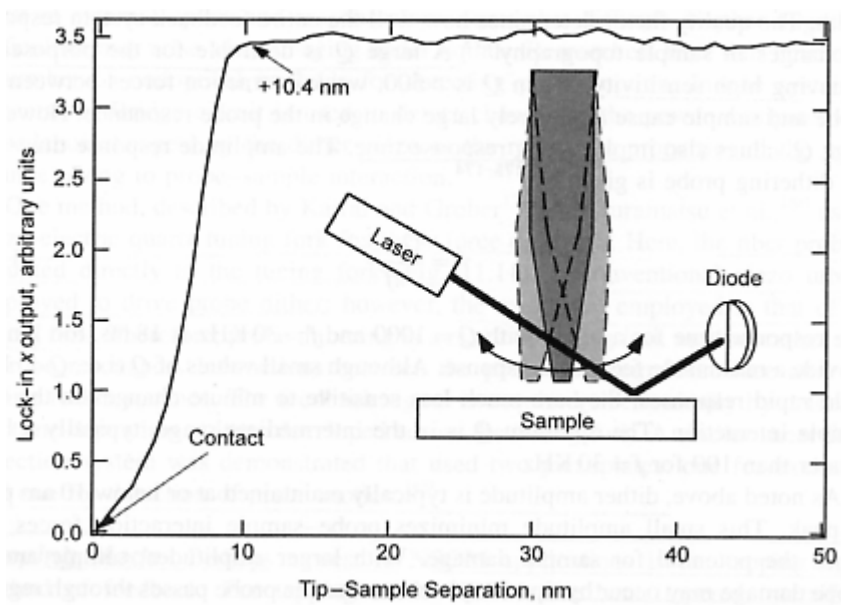

Topography **NSOM Image**

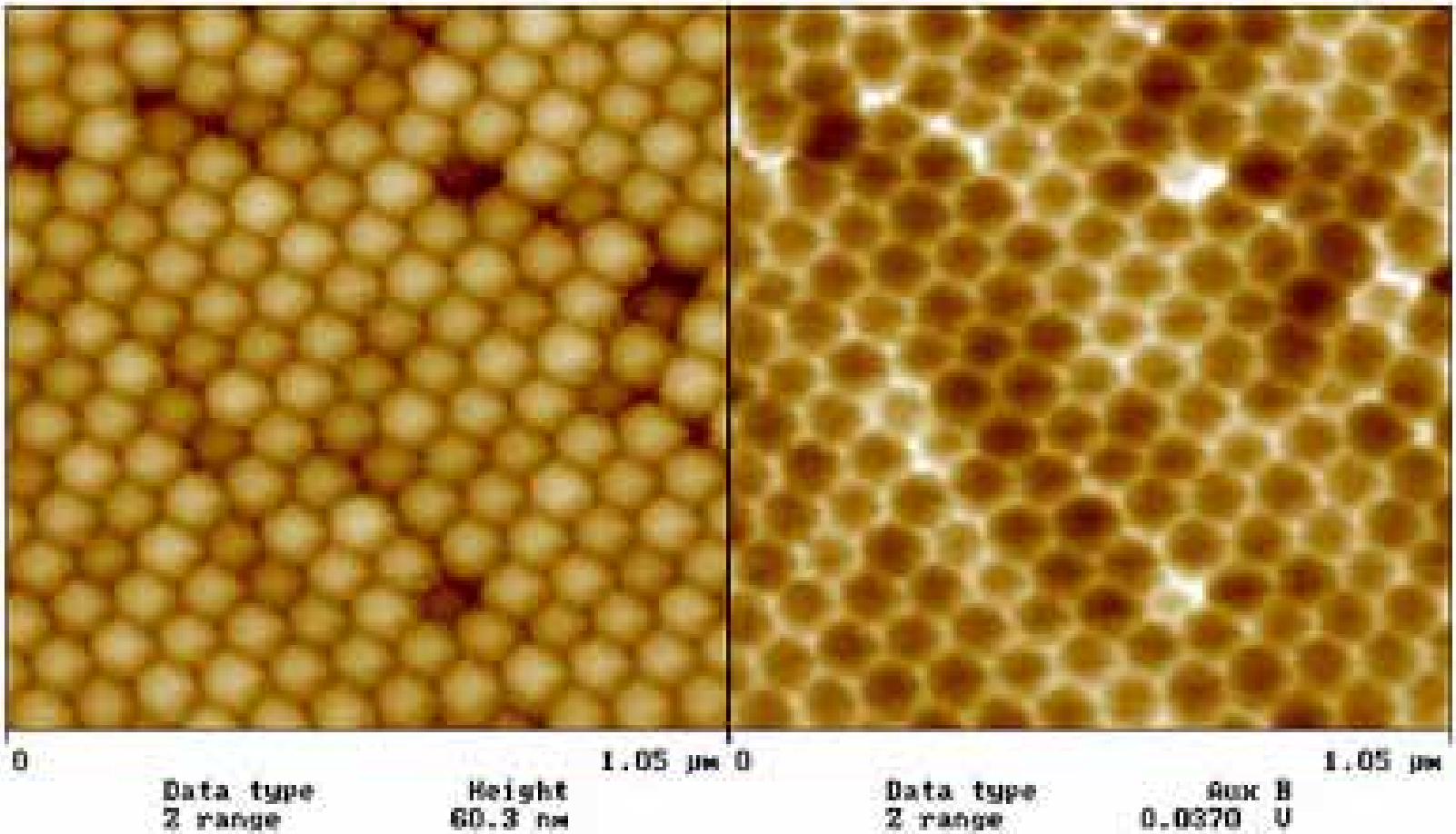

100 奈米直徑之聚苯乙烯顆粒球的原子力顯微 (AFM) 影像 (左) 及穿透式近場光學顯微影像 (右)

Collection-Mode SNOM

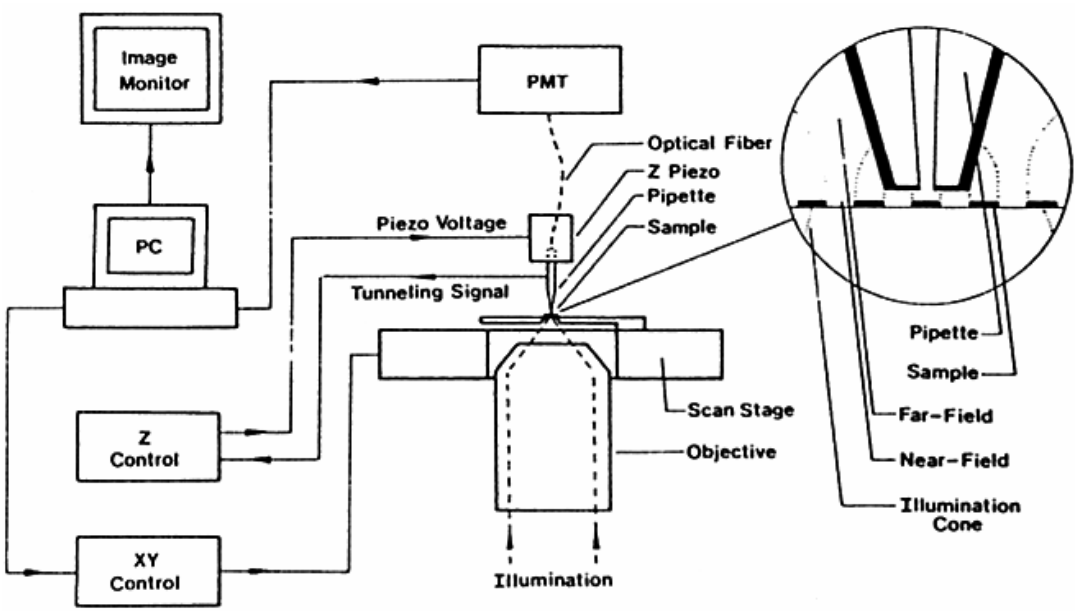

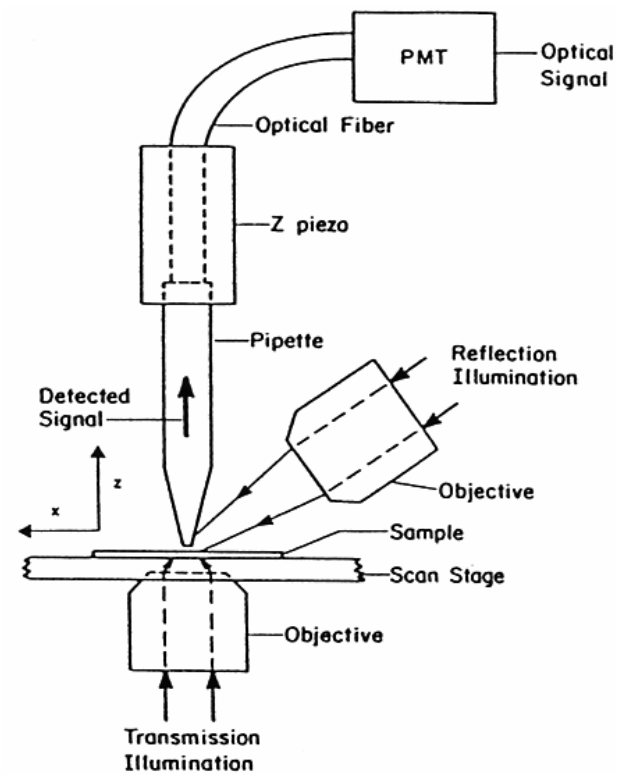

SNOM using cantilever-based metal-coated tips

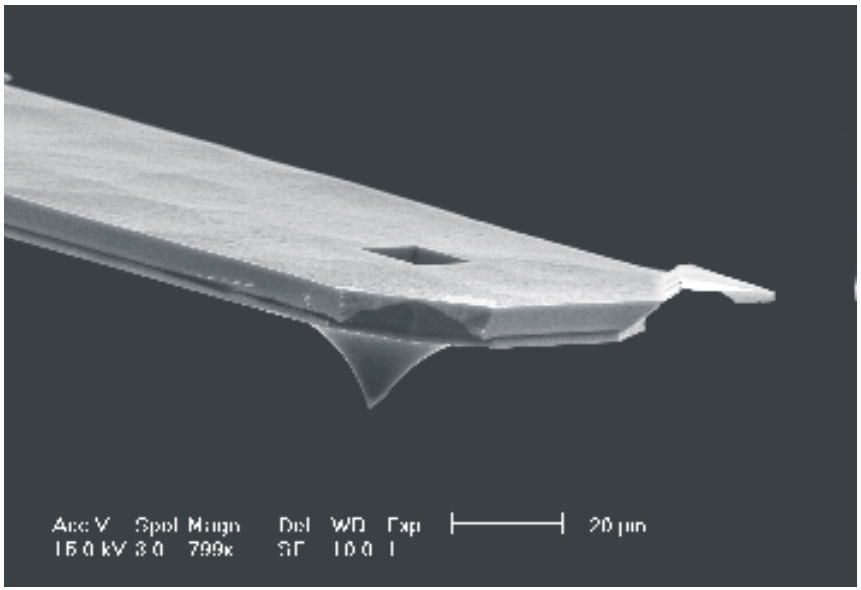

SEM image of a cantilever-based probe having a square hole underneath the tip base.

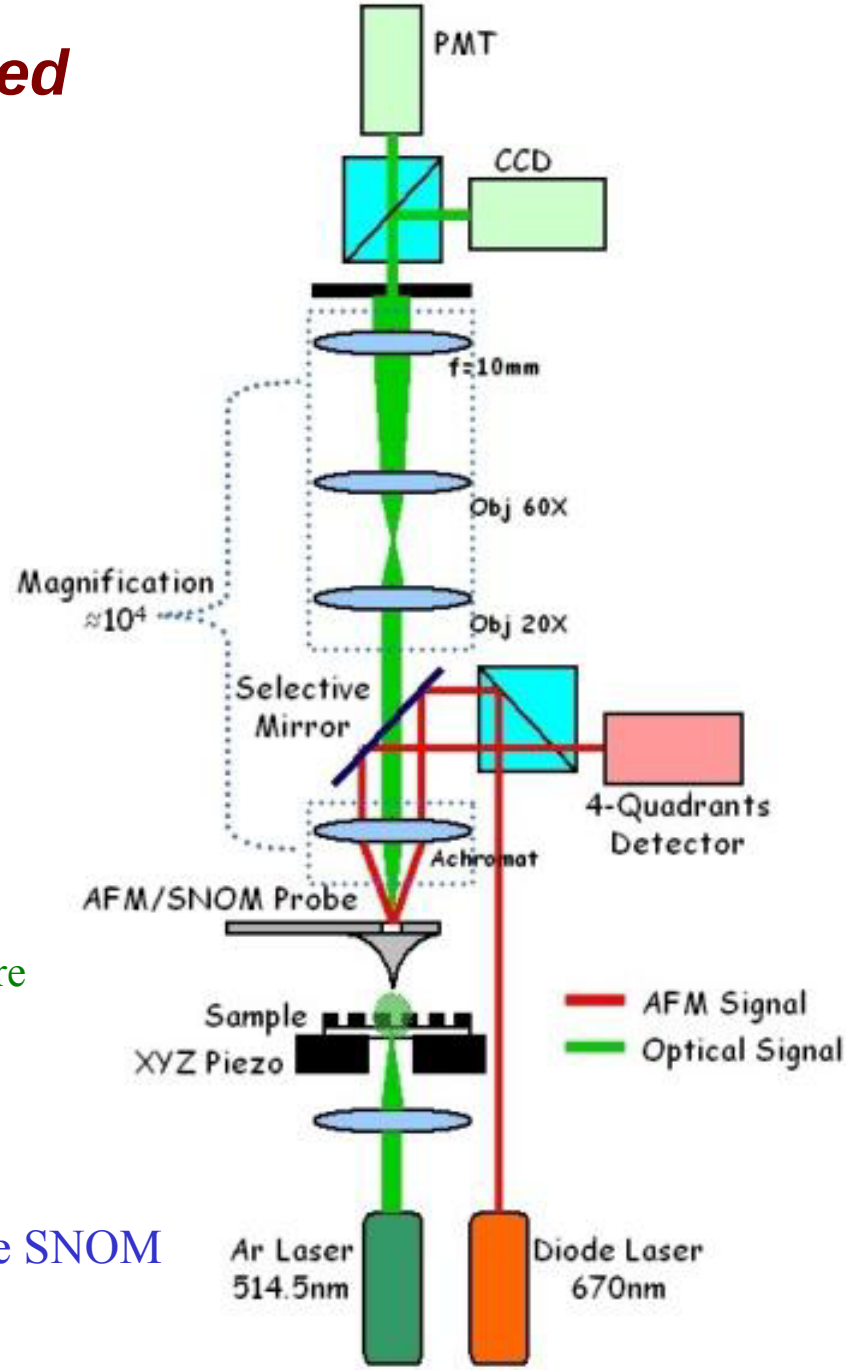

Collection mode SNOM

NSOM Based on a Tuning Fork

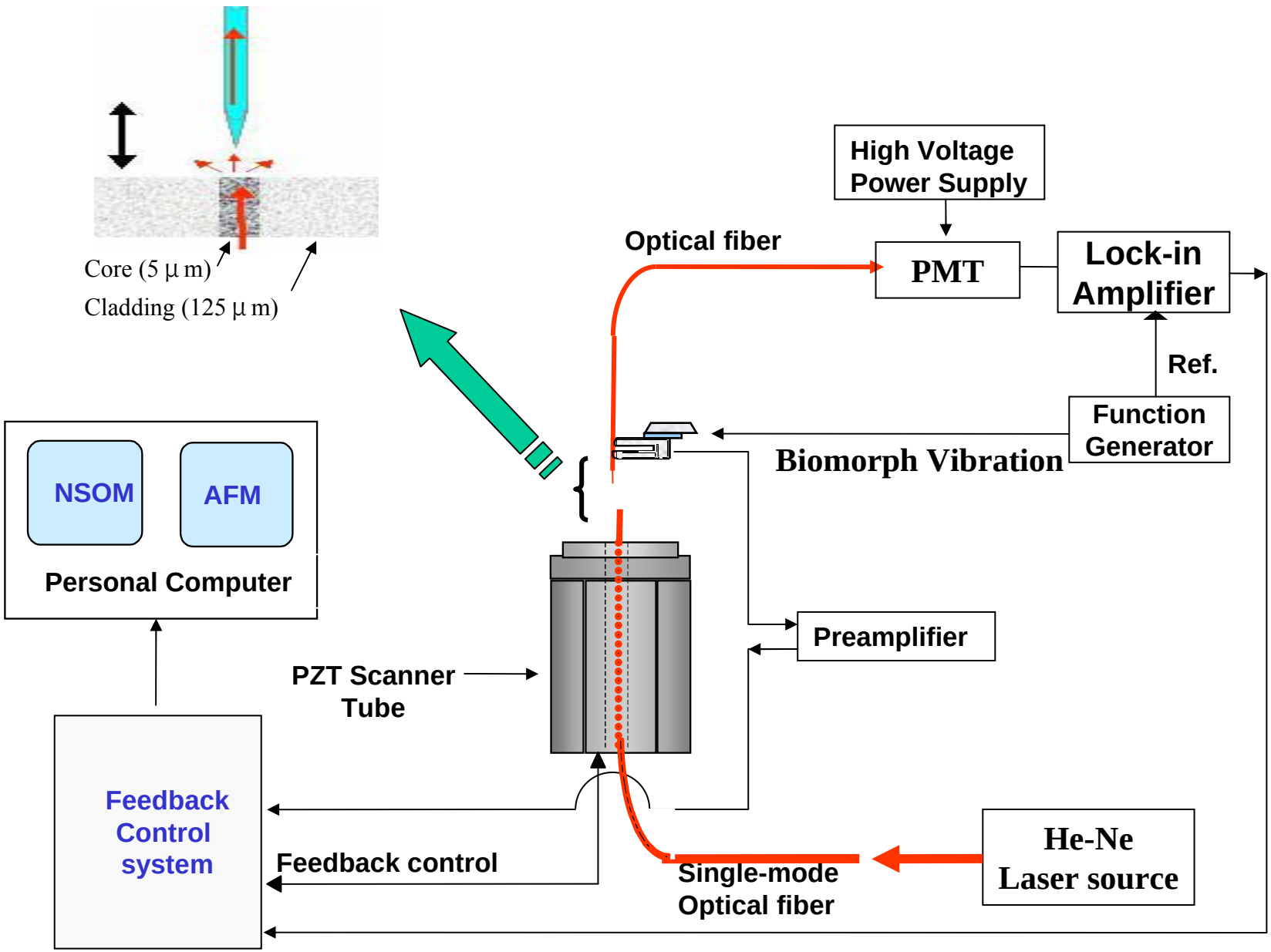

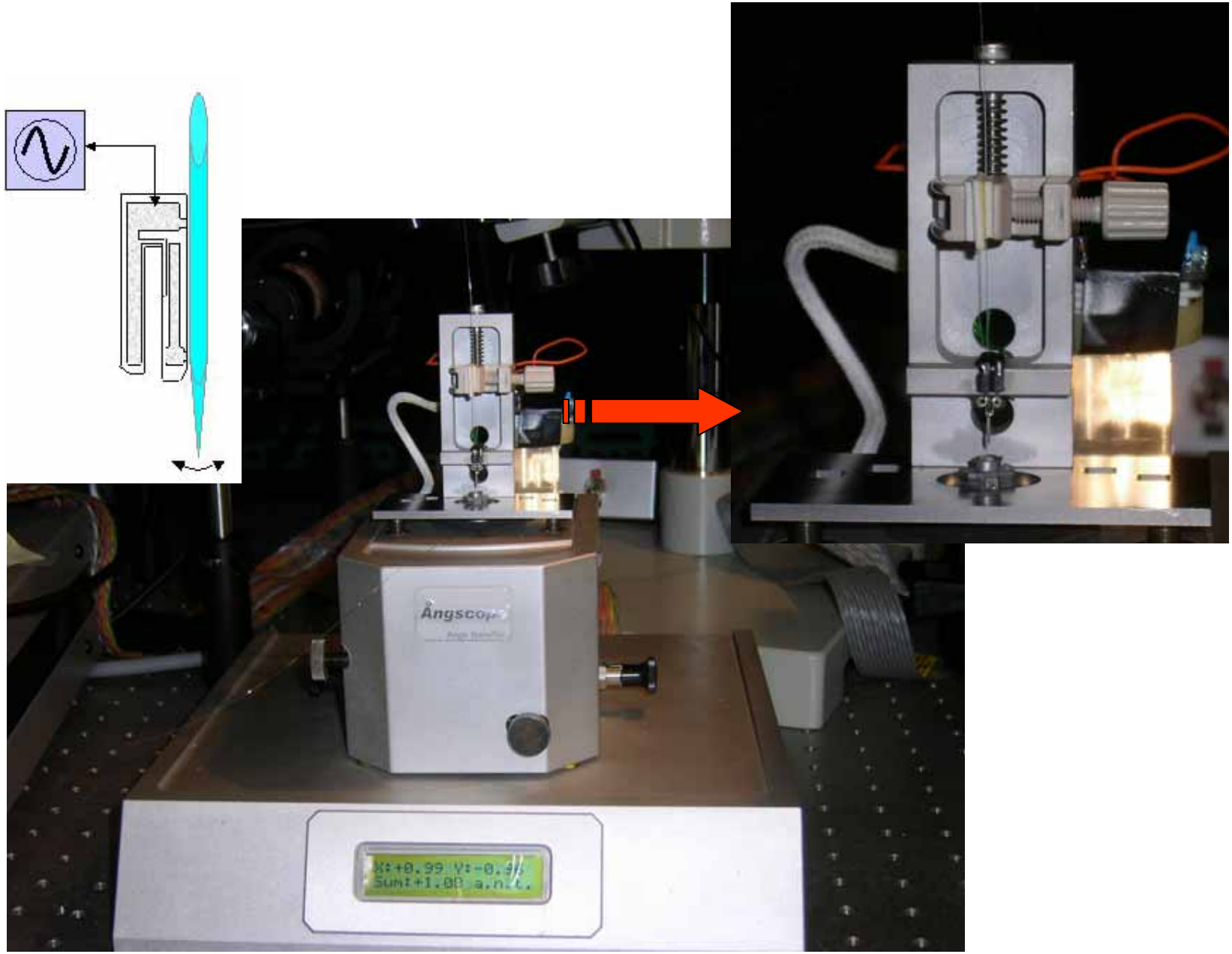
Angscope
X:+0.99 Y:-0.
Sum:+1.00 a.n.t.

AFM Images Taken with a Quartz Tuning Fork

石墨

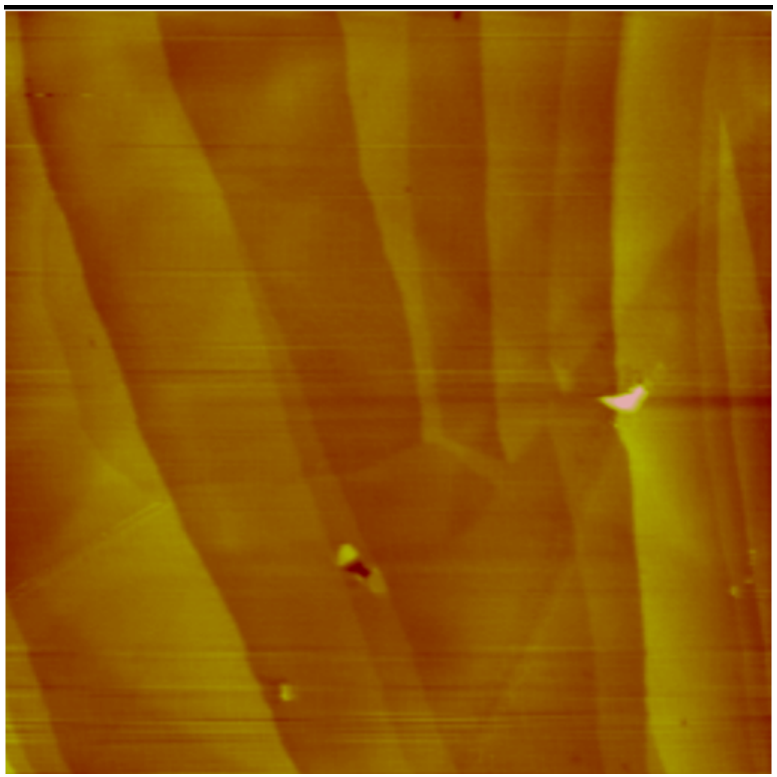

4 μm × 4 μm

標準校正片

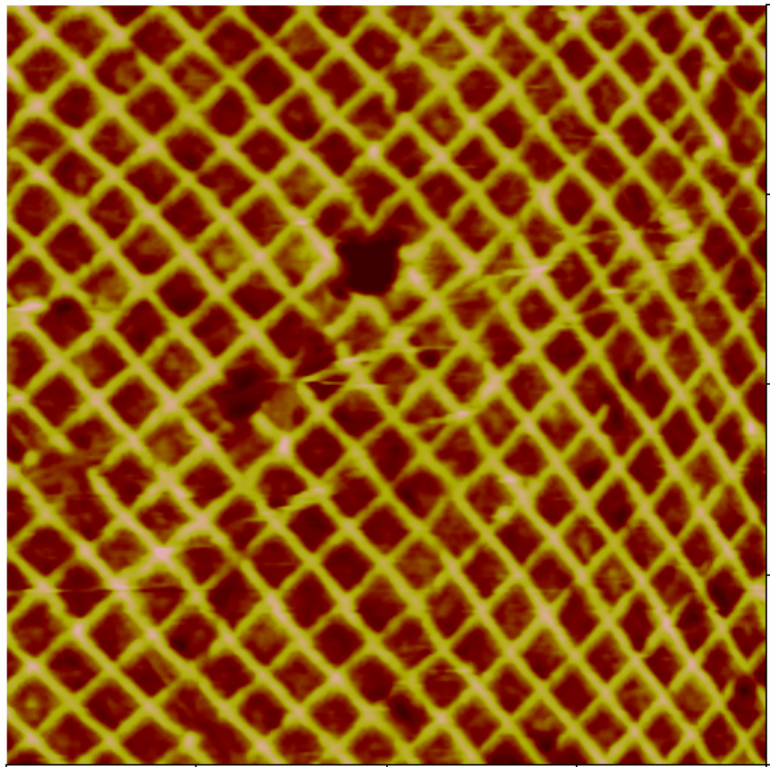

8 μm × 8 μm

Images of an Optical Fiber Core

Single-mode fiber

AFM image (Topography)

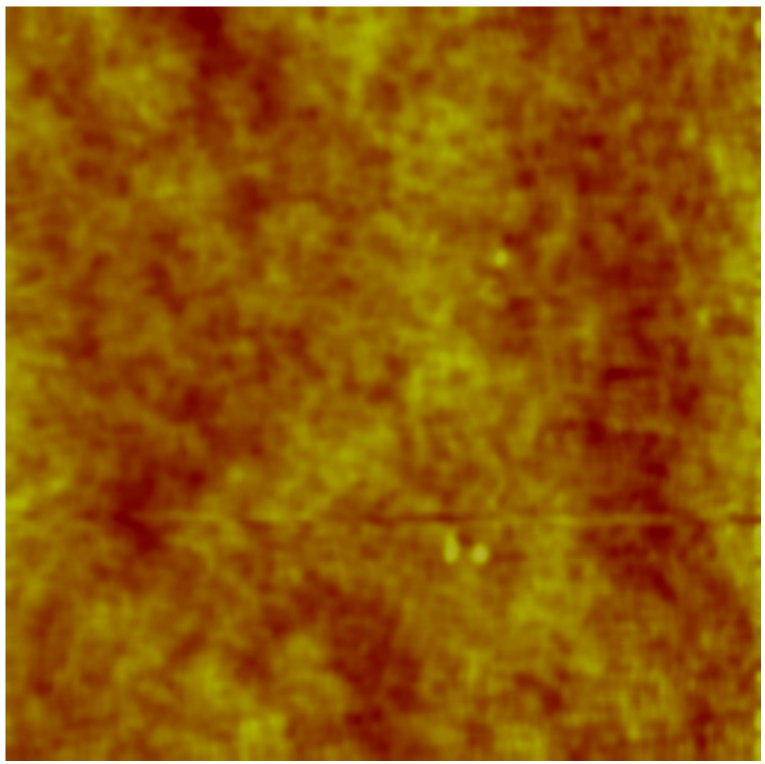

15 μm × 15 μm

NSOM image

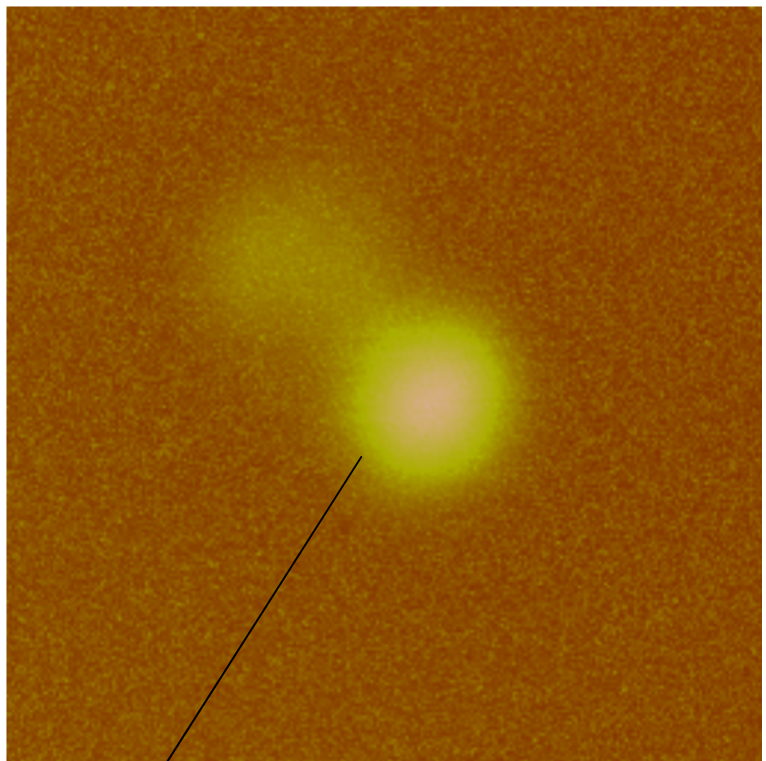

Core area

Single Molecular Fluorescence Imaging

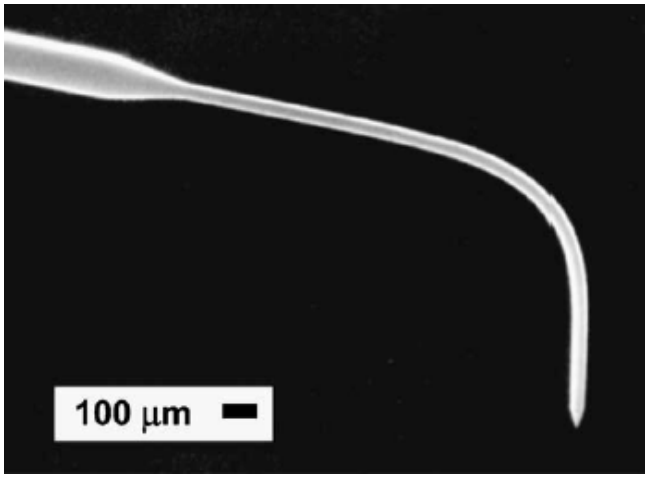

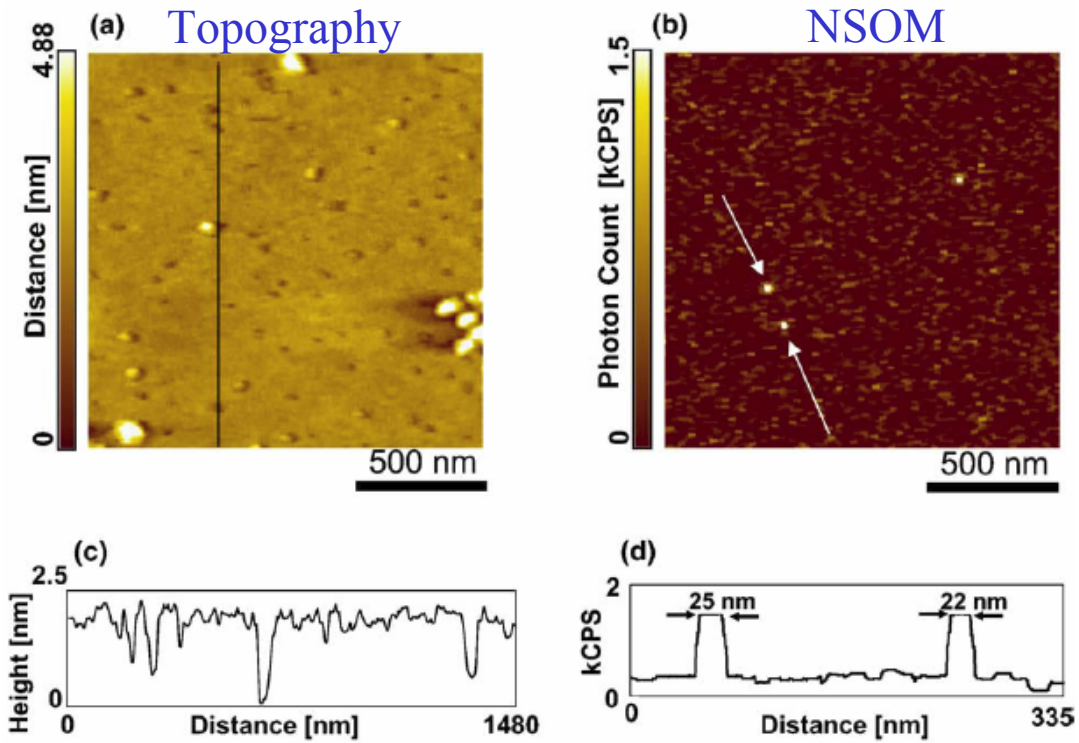

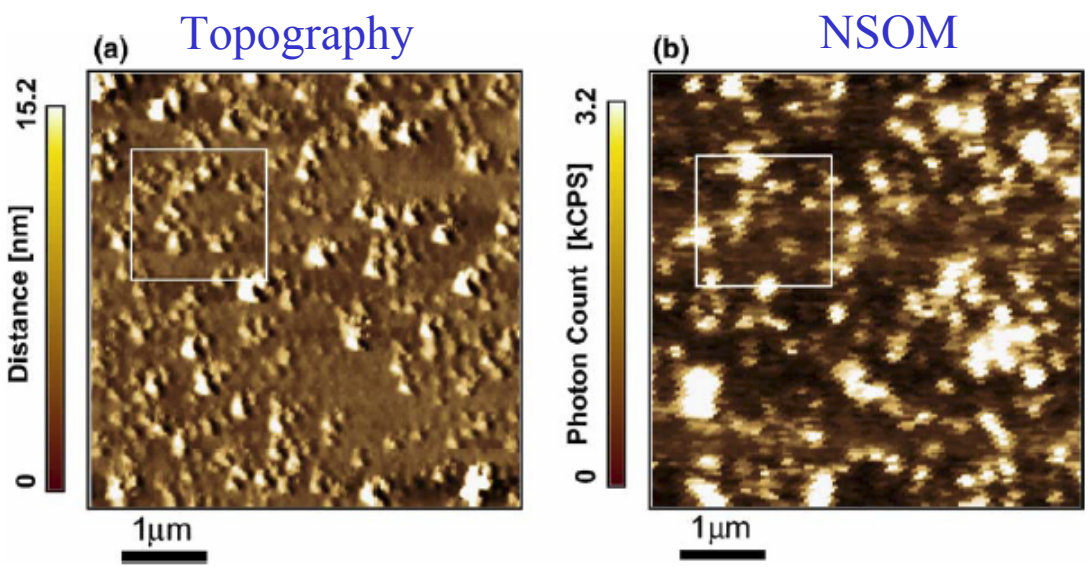

fluorophore, Alexa 532

Illumination mode

Surface Science 549, 273 (2004)

Near-Field Raman Microscopy of Single-Walled Carbon Nanotu

Raman scattering probes the unique vibrational spectrum of the sample and directly reflects its chemical composition and molecular structure. A main drawback of Raman scattering is the extremely low scattering cross section which is typically 14 orders of magnitude smaller than the cross section of fluorescence. Surface enhanced Raman scattering (SERS) induced by nanometer-sized metal structures has been shown to provide enormous enhancement factors of up to 10^{15}.

Topography

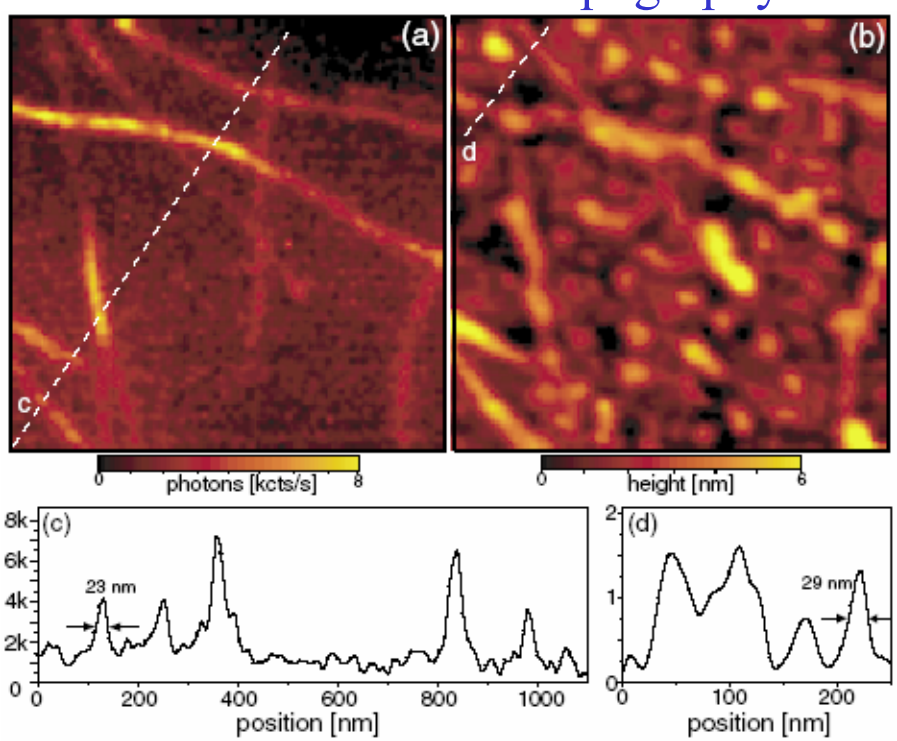

Dependence of the Raman scattering strength of the *G'* band (*I*) on Δz.

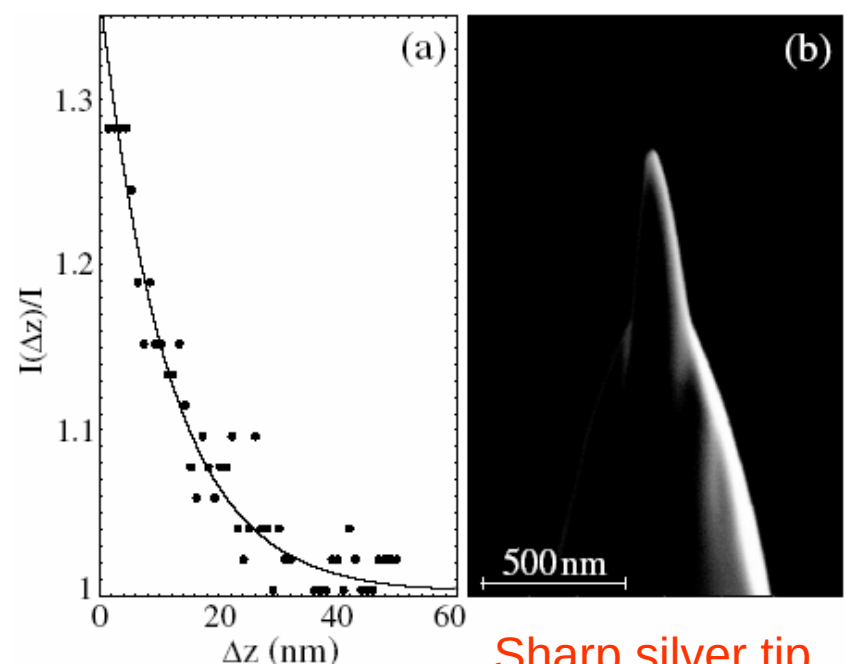

Sharp silver tip

Phys. Rev. Lett. 90, 095503 (2003)